Chapter 4
Introduction to Surface Plasmon Theory

Jean-Jacques Greffet

Abstract This chapter is an introduction to the surface plasmon theory. We start with the solid-state point of view with emphasis on the concept of polariton and the limits of the Drude model. The concept of electromagnetic surface wave is then introduced in a general framework. Three particular cases are then discussed: the surface plasmon, the surface phonon polariton and the Sommerfeld surface wave. The key properties of surface plasmons for optics are discussed in general terms, with special emphasis on the concepts of field confinment and local density of states. The differences between the dispersion relations of surface waves in the presence of losses are analysed and their significance is explained. Finally, an equivalent of the Huygens–Fresnel principle is derived for the surface plasmon polaritons.

4.1 Introduction

This chapter is part of a book devoted to the optics of surface plasmons. The term surface plasmon is used both for polarization oscillation of metallic nanoparticles and for waves propagating along a plane interface and exponentially decaying away from the interface. This chapter will mostly cover the latter case. From the point of view of electrodynamics, surface plasmons are a particular case of a surface wave, a topic that has been extensively covered in the early days of radiowave propagation along the earth [1–4]. From the point of view of optics, surface plasmons are modes of an interface. They have been extensively studied in the 1970s and 1980s. Several excellent monographs are available from this point of view [5–7] and more recent achievements are summarized in Refs. [8–10]. Finally, from the point of view of solid-state physics, a plasmon is a collective excitation of electrons. Excellent introductions can be found in well-known textbooks [11, 12] and in more advanced texts [13–15].

J.-J. Greffet (✉)
Institut d Optique Université Paris-Sud, CNRS, RD 128, F-91127 Palaiseau Cedex, France
e-mail: jean-jacques.greffet@institutoptique.fr

S. Enoch and N. Bonod (eds.), *Plasmonics*, Springer Series in Optical Sciences 167,
DOI: 10.1007/978-3-642-28079-5_4,

The goal of this chapter is to provide an introduction to the three different points of view and to serve as a lecture guide. In the first section, we will show how the plasma frequency can be seen as the natural oscillation frequency of electrons in a thin film. This (solid-state) point of view will be generalized to bulk plasmons in an electron gas in the second section using a hydrodynamic model. This analysis will serve the purpose of explaining the concept of polariton: an electromagnetic wave coupled to a polarization excitation in the material. We will then adopt the macroscopic electrodynamics point of view and derive the dispersion relation of a surface wave. In this approach, the material properties are accounted for by using a dielectric constant without any microscopic model. We will discuss the similarities and differences between different types of surface waves (lateral waves, Zenneck modes, Sommerfeld modes, quasicylindrical waves) without invoking any specific model of the dielectric constant. Hence, this discussion will be equally valid for radio waves or optical waves, for metals or dielectrics. We will then focus on the case of surface plasmon polaritons. To this aim, it is often convenient to use the Drude model but it is also critical to be aware of its limitations. This will be summarized in Sect. 4.5. Surface phonon polaritons and radio surface waves will be introduced in the following sections. In Sect. 4.8, we will outline the key properties that make surface plasmons so unique. The aim of this section is to identify fundamental properties of surface plasmons that may help us to decide when surface plasmons can be useful for optics applications. The subtle issue of the dispersion relation of surface plasmons on lossy materials will be analysed in Sect. 4.9. Finally, surface plasmon optics will be the subject of the last section. It will be shown how the propagation of surface plasmons along a flat interface can be modelled using a Fourier optics framework

4.2 Surface and Particle Electron Oscillation Modes: Introductory Examples

To start, we consider a thin metallic film. The metal is described by a simple model: we assume that there are n free and independent electrons per unit volume. The crystal lattice is modelled by a uniform positively charged background. This is the so-called jellium model. The purpose of this section is to illustrate the essence of a plasmon: it is an oscillatory collective mode of the electrons. To proceed, we assume that classical mechanics can be used.

Let us now assume that a positive static homogeneous electric field $E_{\text{ext}}\hat{\mathbf{x}}$ is applied normally to the film along the x-axis (see Fig. 4.1). A force $-eE_{\text{ext}}\hat{\mathbf{x}}$ is exerted on the electrons so that they will be displaced by x (with $x < 0$). A negative static surface charge nex will appear on the left interface and a positive surface charge on the right side. These surface charges produce a static field that cancels the external field in the metal. Let us now assume that the external electrostatic field is turned off at time $t = 0$. The electrons in the film will be accelerated by the electric field generated by the surface charges. When they return to their initial position, they have acquired a

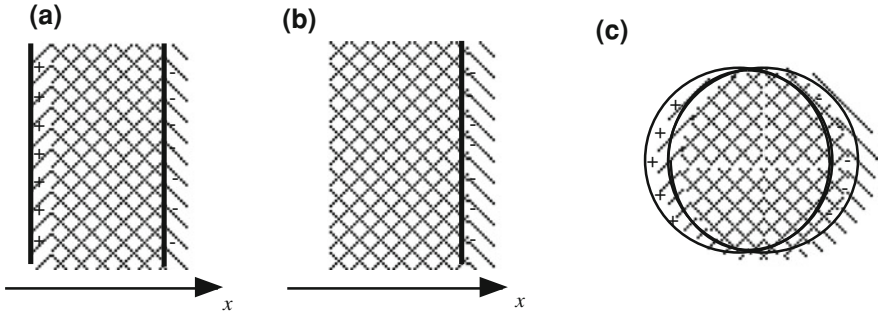

Fig. 4.1 Oscillation of the electron gas for **a** a thin film, **b** a metal–vacuum interface, and **c** a nanosphere

momentum so that they keep moving along the positive x-axis and therefore generate an electric field of opposite sign. This process will be repeated and will produce an oscillation. It is easy to quantitatively describe this phenomenon by using Newton's law applied to a single electron:

$$m\frac{\mathrm{d}^2x}{\mathrm{d}t^2} = -eE_x, \tag{4.1}$$

where we have neglected the magnetic force. Using Gauss's theorem, it can be shown that the field generated by a sheet carrying a surface charge nex is $(nex/2\epsilon_0)\mathbf{u}$ where $\mathbf{u}$ is an outward unit vector. It follows that the field generated by the surface charge nex for a displacement x is found to be $E_x = 2nex/2\epsilon_0$ where the factor 2 accounts for the presence of two interfaces. It follows from Newton's equation that the movement of one electron is given by:

$$\frac{\mathrm{d}^2x}{\mathrm{d}t^2} + \frac{ne^2}{m\epsilon_0}x = 0. \tag{4.2}$$

This simple argument allows us to introduce in a simple way the plasma frequency ω_p:

$$\omega_p^2 = \frac{ne^2}{m\epsilon_0} \tag{4.3}$$

that appears to be the frequency of the collective oscillation of the electrons in the bulk of the film. To summarize, the oscillation is produced by an electric field due to all the electrons. This is why it is called a collective oscillation. With this simple argument, we have captured the essence of the plasmon: *it is the natural collective oscillation of the electrons characterized by the plasma frequency*.

We now consider the case of a single interface. In other words, we consider that the thickness of the film goes to infinity so that the force is only due to the charge density of one interface. It follows that the electric field is due to only one interface

instead of two and takes the value $nex/2\epsilon_0$. The oscillation frequency is therefore $\omega_p/\sqrt{2}$.

We finally consider the case of a nanosphere. For a sphere much smaller than the wavelength, retardation effects can be neglected so that we can use the electrostatic form of the field generated by a uniform polarization field P_x of the particle $E_x = -P_x/3\epsilon_0$ [16]. Inserting this form of the electric field in Eq. (4.1) yields:

$$m\frac{\mathrm{d}^2x}{\mathrm{d}t^2} = -e\frac{-P_x}{3\epsilon_0}. \tag{4.4}$$

The polarization P_x is due to the displacement of the electrons so that we have $P_x = -nex$. Upon inserting this expression in Eq. (4.4), we find:

$$\frac{\mathrm{d}^2x}{\mathrm{d}t^2} + \frac{ne^2}{3m\epsilon_0}x = 0. \tag{4.5}$$

so that the resonance frequency of the plasmon in a nanosphere is given by $\omega_p/\sqrt{3}$.

The modes of a sphere will be further discussed in the chapter written by J. Aizpurua and R. Hillenbrand . In this chapter, we will focus on surface modes that can propagate along a flat interface while decaying exponentially on both sides of the interface. Here, we simply make a comment on terminology. It turns out that both nanosphere modes and modes propagating along an interface are called surface modes although they are different.

4.3 Bulk Plasmon

4.3.1 Hydrodynamic Model: The Concept of Polariton

We now consider a more general analysis of the concept of plasmon. We do not consider a specific geometry. Instead, we look for a general equation describing a charge density wave in an infinite homogeneous electron gas. Our primary objective in this section is to illustrate the concept of polariton in the particular case of a plasmon. The key idea that will be introduced here is that when an electromagnetic wave propagates in a material medium, the field polarizes the medium and therefore excites a mechanical movement of the charges. It follows that field and charges are coupled. This coupled excitation is called a polariton. In the case of a metal, the field can couple to a longitudinal charge density wave that can be viewed as an acoustic wave in the electron gas. The resulting polariton is called a plasmon polariton. In an ionic crystal like NaCl for instance, an electromagnetic field can excite the mechanical motion of the ions (a phonon) and therefore generate a polarization oscillation. This is called a phonon polariton. Finally, the coupling between the field and an electron-hole pair (an exciton) is called exciton polariton. The purpose of this section is to

provide a simple explicit model of this coupling in the case of a metal within the jellium model introduced above. We will use a hydrodynamic model to derive the equation of the charge density wave. To begin, we write Euler's equation, the mass conservation and Gauss–Maxwell equation:

$$\begin{aligned} nm\left[\frac{\partial \mathbf{v}}{\partial t}+\mathbf{v}\cdot\nabla\mathbf{v}\right] &= -ne\mathbf{E}-\nabla P_e, \\ \nabla\cdot(n\mathbf{v}) &= -\frac{\partial n}{\partial t} \\ \nabla\cdot\mathbf{E} &= \frac{n-n_0}{\epsilon_0}(-e), \end{aligned} \tag{4.6}$$

where P_e is the electronic pressure and $n(x,t)$ is the number of electrons per unit volume. We finally introduce the compressibility of the electron gas $\partial P_e/\partial n = mv_F^2/3$ where v_F is the Fermi velocity [12]. When looking for a small amplitude perturbation $n_1(x,t) = n(x,t) - n_0$ and $P_{e1} = P_e - P_{e0}$ where x_0 indicates the equilibrium value of x, the non-linear term $\mathbf{v}\cdot\nabla\mathbf{v}$ can be neglected. Let us comment on this set of equations. For a neutral gas, the electric force $-ne\mathbf{E}$ in Euler's equation would be suppressed. One would then find the usual propagation equation for acoustic waves. Here, after linearizing, we find a set of two coupled linear equations:

$$\begin{aligned} \nabla^2 n_1 - \frac{3}{v_F^2}\frac{\partial^2 n_1}{\partial t^2} &= -\frac{3n_0 e}{mv_F^2}\nabla\cdot\mathbf{E} \\ \nabla\cdot\mathbf{E} &= \frac{n_1}{\epsilon_0}(-e). \end{aligned} \tag{4.7}$$

This system clearly exhibits the coupling between the acoustic wave and the electric field. It is seen that the electron density satisfies a propagation equation with a source term given by the divergence of the electric field. Similarly, the equation describing the longitudinal component of the electric field is driven by the electron density modulation $n - n_0$. The resulting coupled oscillation is called a polariton. The key idea here is that the acoustic and the electromagnetic fields are no longer modes of the system. The mode of the system is a coupled mode called polariton. It can be viewed as an object which is half a photon and half a phonon.

It is now a simple matter to eliminate the electric field and find the propagation equation for the electron density wave that accounts for both the pressure force and the electric force. When searching for a solution of the form $\exp(ikx - i\omega t)$, we find the dispersion relation:

$$\omega^2 = \omega_p^2 + \frac{v_F^2}{3}k^2. \tag{4.8}$$

It turns out that the electric force yields the ω_p^2 contribution, which is much larger than the pressure contribution $v_F^2 k^2$ for wavevectors in the optical regime (i.e. $k \ll \omega/v_F$).

It follows that in the optical regime, the dependence of ω on the wavector can be neglected.

To summarize this section, it has been shown that the plasmon appears to be an acoustic wave in an electron gas. As the particles are charged, an additional electric force has to be accounted for. It turns out that this electric force yields the dominant contribution so that the waves are essentially spatially non-dispersive. Note also that with this approach, it clearly appears that the electric field is parallel to the wavevector as it is due to the charge density gradient.

4.3.2 Bulk Plasmon: Electromagnetic Model

When studying the propagation of waves in a vacuum, we always focus on transverse waves as longitudinal solutions do not exist. This is no longer the case in a material medium. Plasmons are longitudinal solutions of Maxwell equations. In the previous section, we have studied the propagation of coupled mechanical and electromagnetic waves using a hydrodynamic model of a metal. We have found that the electromagnetic solution has an electric field, which is parallel to the wavevector. From a more general perspective, this solution is a longitudinal solution, namely a solution that satisfies $\nabla \times \mathbf{E} = 0$. Such a solution is therefore fully described by the equation $\nabla \cdot \mathbf{D} = 0$. In this section, we examine the existence of a longitudinal solution of Maxwell equations without invoking a specific model of the medium. If we assume that the medium is linear, homogeneous and isotropic, we can introduce a dielectric constant. The most general linear form includes a dependence on the frequency and the wavevector $\epsilon(\mathbf{k}, \omega)$:

$$\mathbf{D}(\mathbf{k}, \omega) = \epsilon(\mathbf{k}, \omega)\mathbf{E}(\mathbf{k}, \omega). \tag{4.9}$$

The dependence of $\epsilon(\mathbf{k}, \omega)$ on ω is called dispersion and the dependence on $\mathbf{k}$ is called spatial dispersion. This dependence on the wavevector leads to a non-local relation between the electric field and the vector $\mathbf{D}$ in direct space so that spatial dispersion and non-local dielectric constant are two aspects of the same property:

$$\mathbf{D}(\mathbf{r}, \omega) = \int \frac{\mathrm{d}\mathbf{k}}{8\pi^3}\epsilon(\mathbf{k}, \omega)\mathbf{E}(\mathbf{k}, \omega)\exp(i\mathbf{k}\cdot\mathbf{r}) = \int \epsilon(\mathbf{r} - \mathbf{r}', \omega)\mathbf{E}(\mathbf{r}', \omega)\mathrm{d}\mathbf{r}'. \tag{4.10}$$

The equation $\nabla \cdot \mathbf{D} = 0$ can be cast in the form:

$$\begin{aligned}\nabla \cdot \mathbf{D} &= \nabla \cdot \int \frac{\mathrm{d}\mathbf{k}}{8\pi^3}\frac{\mathrm{d}\omega}{2\pi}\epsilon(\mathbf{k}, \omega)\mathbf{E}(\mathbf{k}, \omega)\exp(i\mathbf{k}\cdot\mathbf{r} - i\omega t) \\ &= \int \frac{\mathrm{d}\mathbf{k}}{8\pi^3}\frac{\mathrm{d}\omega}{2\pi}\epsilon(\mathbf{k}, \omega)[i\mathbf{k}\cdot\mathbf{E}(\mathbf{k}, \omega)]\exp(i\mathbf{k}\cdot\mathbf{r} - i\omega t) = 0.\end{aligned} \tag{4.11}$$

If we seek a non-zero longitudinal electric field, then $\mathbf{k} \cdot \mathbf{E}(\mathbf{k}, \omega) \neq 0$ so that $\epsilon(\mathbf{k}, \omega) = 0$. A local medium has a dielectric constant that does not depend on $\mathbf{k}$ so that the dispersion relation of the longitudinal solution is given by $\epsilon(\omega) = 0$.

For the particular case of a non-lossy Drude model, $\epsilon(\omega) = \epsilon_0(1 - \omega_p^2/\omega^2)$ so that we find $\omega = \omega_p$ in agreement with the local approximation of Eq. (4.8). The discrepancy with the previous section illustrates the fact that the Drude model is an approximation that does not account for the $\mathbf{k}$-dependence of the dielectric constant. This is usually an excellent approximation as we have discussed above. Yet, it is necessary to be aware that the Drude model is valid, provided that $k \ll \omega_p/v_F$. Models accounting for the k-dependence of the dielectric constant (i.e. non-local models) are discussed in Refs. [12–14, 17].

4.4 Surface Electromagnetic Wave

So far, we have introduced the concept of polariton and the particular case of a bulk plasmon polariton. Let us emphasize that we have only discussed waves propagating in a bulk medium. Moreover, we have studied longitudinal electromagnetic modes. We now consider waves propagating along an interface which are transverse. The aim of this section is to search for a solution confined close to the interface. More precisely, we look for a solution that decays exponentially away from the interface. At this stage, we do not make any particular assumption regarding the specific properties of the medium. Hence, the surface wave dispersion relation that we will find can be applied to any material (e.g. metals, dielectrics) and any frequency range (e.g. radio waves, IR, visible). The only assumption made in what follows is that the media are local and isotropic. Hence, they are characterized by a complex frequency-dependent dielectric constant ϵ_r and a complex frequency-dependent permeability μ_r. We denote the upper medium ($z > 0$) with the index 1 and the lower medium ($z < 0$) with the index 2 as indicated in Fig. 4.2. We denote $\mathbf{k}$ the wavevector and denote (α, β, γ) its Cartesian components and k its modulus.

4.4.1 Dispersion Relation for the Non-Magnetic Case

The electric field obeys the Helmholtz equation in both media:

$$\nabla^2 \mathbf{E}_i + \mu_i \epsilon_i \frac{\omega^2}{c^2} \mathbf{E}_i = 0, \tag{4.12}$$

with $i = 1, 2$. For a p-polarized solution (also called TM for transverse magnetic), we seek a solution of the form:

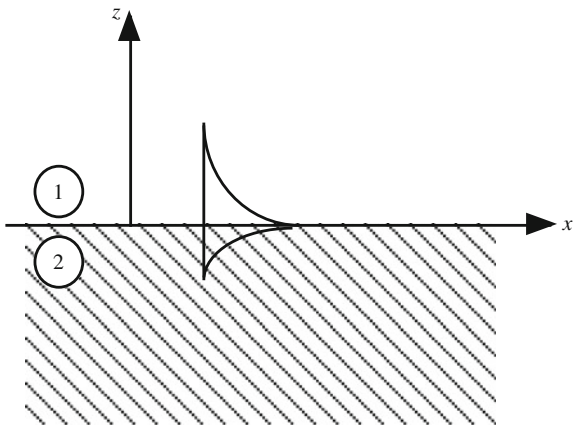

Fig. 4.2 Schematic representation of the exponential decay along z of the amplitude in media *1* (dielectric) and *2* (metal) of a surface wave propagating along the x-axis

$$\begin{aligned} z > 0 \quad & E_{x1} = E_0 \exp[i\alpha x + i\gamma_1 z] \\ z < 0 \quad & E_{x2} = E_0 \exp[i\alpha x - i\gamma_2 z] \end{aligned} \tag{4.13}$$

that satisfies the continuity condition along the interface. Here,

$$\gamma_1 = [\mu_1 \epsilon_1 \omega^2/c^2 - \alpha^2]^{1/2} \tag{4.14}$$

with $Im(\gamma_1) > 0$ and

$$\gamma_2 = [\mu_2 \epsilon_2 \omega^2/c^2 - \alpha^2]^{1/2} \tag{4.15}$$

with $Im(\gamma_2) > 0$ so that the waves decay exponentially far from the interface. We look for transverse waves so that, by definition, $\nabla \cdot \mathbf{E} = 0$. In Fourier space, this relation becomes $\mathbf{k} \cdot \mathbf{E} = 0$ where $\mathbf{k} = (\alpha, 0, \gamma)$. We stress that this equation does not have the usual geometrical meaning of two perpendicular real vectors because $\mathbf{k}$ is complex. In other words, transverse (i.e.$\nabla \cdot \mathbf{E} = 0$) should not be confused with perpendicular. It follows that:

$$\begin{aligned} z > 0 \quad & E_{z1} = -\frac{kE_0}{\gamma_1} \exp[i\alpha x + i\gamma_1 z] \\ z < 0 \quad & E_{z2} = \frac{kE_0}{\gamma_2} \exp[i\alpha x - i\gamma_2 z]. \end{aligned} \tag{4.16}$$

If we now enforce the continuity condition of the z-component of $\epsilon\mathbf{E}$ at the interface, we obtain:

$$\epsilon_1 \gamma_2 = -\epsilon_2 \gamma_1. \tag{4.17}$$

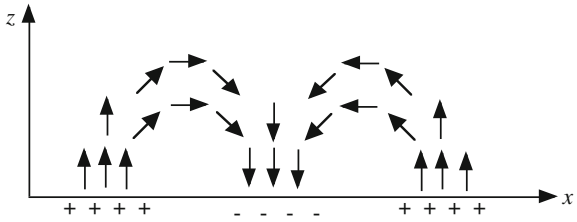

Fig. 4.3 Polarization of the surface plasmon polariton. The figure illustrates the surface charge density wave. It follows that the electric field has a normal component at the interface that oscillates. The figure shows that the continuity of the field in the vacuum requires a curvature of the field lines. The electric field is thus elliptically polarized in the plane (x, z)

These equations are the dispersion relations of the surface wave. To obtain a more explicit form, we take the square of both terms. Note that we lose the sign at this point so that we will need to check that the final solution satisfies the original dispersion relation. For TM-polarization, the solution for α is denoted as $K_{SP}(\omega)$ and is given by:

$$K_{SP}^2(\omega) = \frac{\omega^2}{c^2}\frac{\epsilon_1\epsilon_2}{\epsilon_1 + \epsilon_2}. \tag{4.18}$$

A similar calculation for the magnetic case in s-polarization yields:

$$\mu_1\gamma_2 = -\mu_2\gamma_1. \tag{4.19}$$

4.4.2 Polarization of the Surface Wave

We have seen that the electric field of a surface wave propagating along the x-axis has two components along the x and the z axes. Moreover, the z-component of the electric field is complex. Hence, the electric field has an elliptic polarization in the (x, z) plane. This peculiar polarization can be understood from the following remark. The existence of a z-component of the electric field entails the presence of a surface charge $P_{z2} - P_{z1}$ along the interface. Hence, the surface wave can be viewed as a surface charge density wave propagating along the x-axis as depicted in Fig. 4.3. Since in the vacuum above the interface the field lines must be continuous, there must be an x-component of the field to close the line fields (see Fig. 4.3).

It is worth emphasizing a difference between the current density and the surface charge associated with the surface plasmon. Although the current density $\mathbf{j} = -i\omega\mathbf{P} = -i\omega\epsilon_0(\epsilon_2 - 1)\mathbf{E}$ penetrates in the metal over the skin depth, the surface charge does not penetrate in the metal as $\nabla \cdot \mathbf{P} = \epsilon_0(\epsilon_2 - \epsilon_1)\nabla \cdot \mathbf{E} = 0$ below the interface. The contribution to the surface charge is a pure surface term given by $P_{z2} - P_{z1}$. For a metal–vacuum interface, it is simply given by P_{z2}. From a physical

Table 4.1 Decay length for a surface plasmon propagating along a gold/vacuum interface

λ_i (μm)	0.633	1	10	36
δ_x	9.8	91.6	38,880	504,243
δ_{z1}	0.165	0.51	57.3	702.67
δ_{z2}	0.014	0.012	0.011	0.013

Data taken from Etchegoin et al. at 633 nm and 1 μm [19], from Ordal et al. [20] for 10 and 34 μm

point of view, a surface charge must have some finite extension along the z-axis. One has to account for non-local effects to introduce the relevant length scale. It is the Thomas–Fermi length scale, which is of the order of tenths of nm.

4.4.3 Length Scales of a Surface Wave

There are three different lengths characteristic of a surface wave. It is seen from Eq. (4.18) that the wavevector is complex if there are losses. The imaginary part of K_{SPP} accounts for the decay of the surface wave upon propagation along the interface. A characteristic decay length can be defined by $\delta_x = 1/Im(K_{SPP})$. As the wave does not radiate, the decay is entirely due to losses in the media. In other words, the surface wave energy is converted into heat. There are two other characteristic lengths accounting for the exponential decay of the surface wave away from the interface. They are given by $\delta_{zi} = 1/Im(\gamma_i)$ in medium i. They are found by inserting Eq. (4.18) into Eqs. (4.14, 4.15):

$$\frac{1}{\delta_{zi}} = Im[\gamma_i] = \frac{\omega}{c} Im\left[\frac{\epsilon_i^2}{\epsilon_1 + \epsilon_2}\right]^{1/2} \tag{4.20}$$

Typical orders of magnitude for metals are given in Table 4.1. It is clearly seen that the surface plasmon has a decay length along the x-axis of the order of a few micrometers in the visible range, but considerably larger in the infrared. Regarding the spatial extension of the wave in the metal (medium 2), it is seen that the decay length is almost constant. It is mainly given by the skin depth in the metal and is of the order of 12 nm. By contrast, the extension of the surface wave given by δ_{z1} in medium 1 changes dramatically. It varies between 165 nm in the visible and 700 μm in the IR. Hence, it is seen that the surface wave is not confined close to the interface in the IR. Since most of the energy of the mode is in the vacuum, Joule losses are negligible so that the decay length upon propagation is drastically reduced.

We finally note that the confinment in a dielectric is due to the fact that $\alpha^2 > \epsilon_1 \omega^2/c^2$. We note in particular that for very large wavevectors α, $\delta_{zi} = 1/Im(\gamma_i) \approx 1/\alpha$, so that large vectors are strongly confined.

4.4.4 Link with Resonances of the Reflection Factor

An alternative approach to find the dispersion relation consists in looking for the poles of the Fresnel reflection factor. The reason for looking at the Fresnel factors is simple. Since we can write $E_r^{s,p} = r_{s,p} E_{inc}^{s,p}$, it is seen that the reflection factor $r_{s,p}$ can be considered to be a linear response factor to the incident field $E_{inc}^{s,p}$ viewed as an external excitation. As for any linear system, a resonant response is the signature of the excitation of a mode of the system. Hence, writing that the denominator of $r_{s,p}$ is zero yields the pole, which is the signature of a mode of the interface. It can be checked that $\epsilon_1\gamma_2 + \epsilon_2\gamma_1$ is indeed the denominator of the Fresnel reflection factor for p-polarization for a non-magnetic material. We can now generalize the approach to a magnetic material for both polarizations. The Fresnel reflection factors can be cast in the form:

$$r_s = \frac{\mu_2\gamma_1 - \mu_1\gamma_2}{\mu_2\gamma_1 + \mu_1\gamma_2}; \quad r_p = \frac{\mu_1\epsilon_2\gamma_1 - \mu_2\epsilon_1\gamma_2}{\mu_1\epsilon_2\gamma_1 + \mu_2\epsilon_1\gamma_2}. \tag{4.21}$$

It follows that the corresponding dispersion relation can be written as follows:

$$\mu_2\gamma_1 + \mu_1\gamma_2 = 0; \quad \mu_1\epsilon_2\gamma_1 + \mu_2\epsilon_1\gamma_2. \tag{4.22}$$

It is seen that a surface wave can be obtained in the case of a magnetic material in s-polarization if the permeabilities μ_i have opposite signs. It is also of interest to note that the zeros and the poles of the reflection factor are given by very similar equations. We will come back to this point in the section on surface plasmons. This approach is of particular interest when dealing with more complex systems such as multilayers. It does account for guided modes, interface modes and the coupling between these modes.

A technical remark might be useful here. The reader may be familiar with a presentation of the Fresnel reflection factor using the incident angle θ_i as a variable instead of the parallel component of the wavevector k. For the case of a propagating incident wave in a lossless dielectric medium with refractive index n_1, it is essentially a matter of taste to use k or $n_1(\omega/c)\sin\theta_i$. If we seek the zero of the denominator, we need to use a real value of k, which is larger than $n_1\omega/c$. A question then arises: is such a large k physical? If yes, how can we generate a large surface wavevector?

4.4.5 Generation of a Surface Wave

When using the Fourier representation of a field, a real wavector k is used. It is known that in a vacuum, the wavevector has a modulus ω/c so that it might seem that large values of k are not possible. It might be useful at this point to write the Fourier expansion of a scalar spherical wave propagating with phase velocity c known as Weyl's expansion:

$$\frac{\exp(ikr)}{r} = 2i\pi \int_{-\infty}^{\infty} \frac{\mathrm{d}\alpha}{2\pi} \int_{-\infty}^{\infty} \frac{\mathrm{d}\beta}{2\pi} \frac{1}{\gamma} \exp[i(\alpha x + \beta y + \gamma|z|)], \tag{4.23}$$

where $\gamma = [\omega^2/c^2 - \alpha^2 - \beta^2]^{1/2}$ and $Im(\gamma) > 0$. This mathematical identity clearly exhibits the fact that a spherical scalar wave produced by a point-like source contains arbitrarily large values of α and β. Due to the dispersion relation $\alpha^2 + \beta^2 + \gamma^2 = \omega^2/c^2$, it is seen that γ is imaginary for $\alpha^2 + \beta^2 > \omega^2/c^2$. Hence, the field produced by a point-like source contains evanescent waves that always decay away from the source as indicated by the absolute value $|z|$. Placing a point-like source above an interface amounts to illuminate this interface with decaying evanescent waves. There are other techniques to generate evanescent waves, i.e. to generate large wavevectors.

(1) One can use a metal film with a thickness smaller than the skin depth separating two dielectric media with different dielectric constants n_1 and $n_2 > n_1$. Here, the key idea is to take advantage of a large refractive index to increase the modulus of the wavevector. By illuminating from the side of the high refractive index medium, it is possible to excite through the film with a plane wave with wavevector $\alpha = n_2\omega/c \sin(\theta_i)$ and excite the surface wave on the other side by taking adavantage of the fact that the incidence angle can be chosen so that $\alpha > n_1\omega/c$.
(2) A grating with period d can be used so that the nth order of the grating has a wavevector $\alpha_n = n_1\omega/c \sin\theta_i + n2\pi/d$ that can be equal to k_{sp}.

4.5 Surface Plasmon Polariton

In this section, we will consider the specific case of surface waves propagating at the interface between a metal and a dielectric. These surface waves are called surface plasmon polaritons. Some authors [6, 8] call surface plasmons the electrostatic limit (or large wavevector limit) of the surface plasmon polariton as introduced in the previous section. However, most authors use the term "surface plasmon" as a generic term without making this distinction.

4.5.1 Dielectric Constant of a Metal

Drude model

We start the discussion by introducing the Drude model of the dielectric constant for a metal described by an electron gas. The relative dielectric constant can be cast in the form:

$$\epsilon_r(\omega) = 1 - \frac{\omega_p^2}{\omega^2 + i\gamma(\omega)\omega}. \tag{4.24}$$

This relation clearly shows that there is a strong frequency dependence (i.e. dispersion) of the dielectric constant. Since the Fourier transform of a product is a convolution product, the relation $\mathbf{D}(\mathbf{r}, \omega) = \epsilon_0\epsilon_r(\omega)\mathbf{E}(\mathbf{r}, \omega)$ becomes in time domain:

$$\mathbf{D}(\mathbf{r}, t) = \int_{-\infty}^{t} \epsilon_0\epsilon_r(t - t')\mathbf{E}(\mathbf{r}, t')dt'. \tag{4.25}$$

Two time scales are included in the model. On the one hand, the plasma frequency is the mode frequency of the charge density oscillation. The plasma frequency lies in the near ultraviolet for most metals. A second time scale appears in this formula, namely the relaxation time $\tau(\omega) = 1/\gamma(\omega)$. The relaxation time describes the relaxation processes for excited electrons. A major source of confusion is that in most references, the dependence of the relaxation coefficient on the frequency ω is omitted. Care must be taken as the relaxation of an electron with an energy of a few eV has little in common with the relaxation of an electron with an energy of few meV. The decay processes are completely different. It follows that it is not correct to insert in the model of optical properties the value of γ derived from the conductivity at zero frequency. In particular, it is known that γ at zero frequency decays when the temperature decays. However, this is not a valid conclusion in the optics regime. Indeed, even at low temperature, the electron–electron interaction remains an efficient relaxation channel and is almost not dependent on the electron temperature. In addition, electrons can emit phonons. These two mechanisms are still possible at low temperature. One of the practical conclusions of this paragraph is that metal losses cannot be significantly reduced when reducing the temperature. The reader will find more information on electron losses in Refs. [21–26]. Finally, we mention that the relaxation time is typically of the order of 10 fs for noble metals and visible excitations.

Beyond the Drude model

Although the Drude model can be a very useful tool, it is important to keep in mind that its accuracy is much better in the IR than in the visible range. The reason is that the Drude model accounts for the contribution of the free electrons in the conduction band. When the frequency increases, photons can excite electrons in electronic bands of lower energies (usually a d-band) so that new absorption channels are available. This introduces serious deviations from the Drude model. This can be accounted for by developing fits of the measured dielectric constant as reported in several references [19, 27–29]. It is of course essential to use these realistic models when studying plasmons using time-domain calculations. Figure 4.4 illustrates the large difference in the optical part of the spectrum between a Drude model obtained by

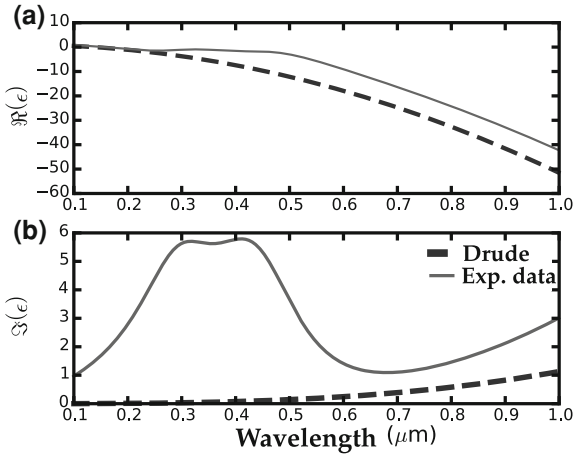

Fig. 4.4 Comparison of experimental data and a Drude fit of the dielectric constant for gold **a** real part of the dielectric constant **b** imaginary part of the complex dielectric constant

fitting experimental data and a more detailed fit of the data reported by Johnson and Christy for gold [30]. The absorption band observed in the imaginary part of the dielectric constant between 0.3 μm and 0.4 μm is due to absorption by d-band electrons.

Another limitation of the Drude model is that it does not account for non-locality also called spatial dispersion. Spatial dispersion means that the dielectric constant depends on the wavector. In direct space, the polarization at point **r** depends not only on the value of the electric field at this point but also in its vicinity, hence the name non-locality [18]. The dielectric constant has two length scales corresponding to two different phenomena. The first effect is the screening of the field at an interface. Classical local electromagnetism assumes that the normal component is divided by ϵ_r at the interface between a vacuum and a metal. The microscopic phenomenon responsible for this effect is the screening of the field by the electrons. It requires a certain length to take place. This screening length is the so-called Thomas–Fermi length for metals. For electrolytes, the corresponding screening length is called Debye–Huckel length. This phenomenon corresponds to longitudinal fields. We now consider the second length scale that appears in non-local models of the optical response of metals. This length scale is the length travelled by an electron at velocity v_F during an optical cycle. When this length scale is much smaller than the wavelength, the optical properties are not affected. By contrast, for wavectors $k > \omega_p/v_F$, non-local corrections are expected. This can be understood from the hydrodynamic model introduced in Sect. 4.3.1. It is seen from that model that the term $v_F^2 k^2$ becomes dominant for large values of k. This condition also corresponds to a threshold for energy absorption. It can be understood in two different ways. The first picture is due to Landau and has been introduced to explain the absorption in plasmas. When the electron velocity v_F is equal to the phase velocity ω/k of the field, the electron velocity and the field are always in phase so that the energy transfer is very efficient. This is the so-called Landau damping mechanism.

Another point of view is to consider that the absorption of a plasmon allows generating an electron hole-pair. There is a threshold value of k due to momentum conservation. Let us consider an interaction between an electron with initial momentum $\hbar q$ and initial energy $\hbar^2 q^2/2m$ with a surface plasmon with energy $\hbar\omega$ and momentum $\hbar k$. The electron is close to the Fermi surface so that $\hbar q = m v_F$. The interaction must conserve the energy and the momentum so that we have

$$\begin{aligned} \hbar\omega &= \frac{\hbar^2}{2m}\left[(\mathbf{q}+\mathrm{d}\mathbf{q})^2 - \mathbf{q}^2\right] \approx \frac{\hbar^2 q \mathrm{d}q}{m} \approx \hbar v_F \mathrm{d}q, \\ \hbar\mathbf{k} &= \hbar\,\mathrm{d}\mathbf{q} \end{aligned} \tag{4.26}$$

where we have given a rough estimate of $\hbar\omega$. Eliminating $\mathrm{d}q$ between the two equations, it is seen that for $k \approx \omega/v_F$, the interaction satisfies energy and momentum conservation. For usual electromagnetic excitations, this process is forbidden as the electromagnetic wavevector $k \approx \omega/c$ is too small. Yet, surface plasmons may have large wavevectors and therefore this process can take place. We note here that this process can also take place when a dipole is close to a metal interface at a distance d smaller than v_F/ω as its near-field contains large wavevectors. In summary, for values of k larger than ω/v_F, the plasmon is damped as it can relax by generating an electron-hole pair. Clearly, this process introduces a cut-off spatial frequency for the surface plasmons. More information on the non-local description of the optical properties of solids can be found in Refs. [12–14, 17]. For noble metals, the typical Thomas–Fermi screening length is of the order of 0.1 nm and the typical Landau damping length scale is of the order of 1 nm.

4.5.2 Dispersion Relation of a SPP

Non-Lossy Drude Metal

In this section, we discuss the dispersion relation of a surface plasmon using the discussion on the Drude model. As already stated, this is a crude model for noble metals when the frequency approaches the plasma frequency. We nevertheless use it for the sake of simplicity to discuss a few key issues. Although losses play a very important role, we start by neglecting them in order to base our introductory discussion on the simplest analytical formulas. However, we emphasize that the results obtained are only a rough approximation of the actual properties. We consider that the upper medium is a dielectric with a real dielectric constant ϵ_1 and the lower medium is a metal described by a non-lossy ($\gamma = 0$) Drude model.

Inserting the Drude form of the dielectric constant in the dispersion relation given by Eq. (4.18), we obtain:

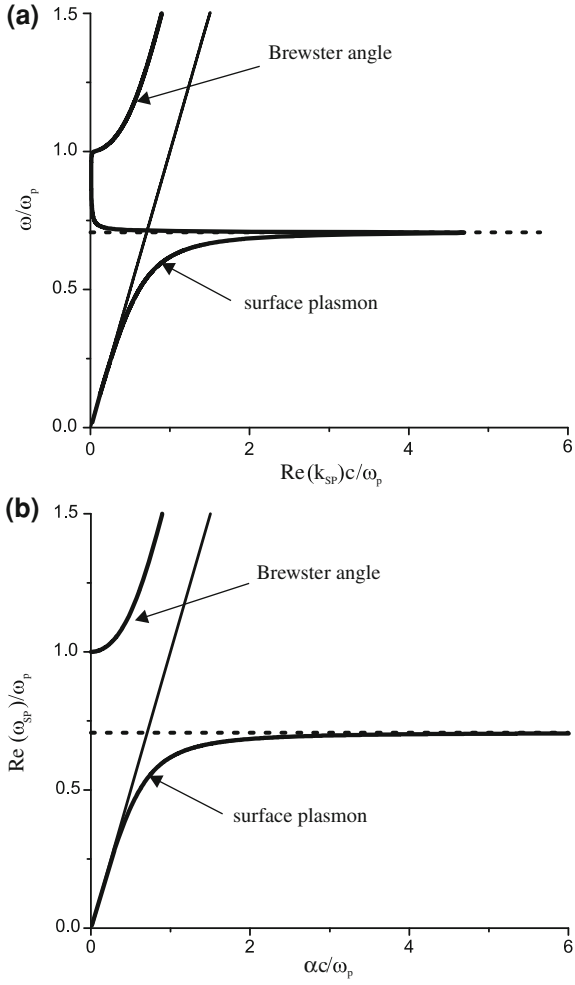

Fig. 4.5 Dispersion relation of a surface plasmon propagating along an interface separating a lossy metal described by the Drude model from a vacuum. The implicit dispersion relation can be solved searching for a real frequency and a complex wavevector or vice versa. Two different dispersion relations are obtained. **a** Frequency versus real part of the complex value of k_{sp}, **b** real part of the complex frequency versus the real wavevector α.

$$k_{sp} = \frac{n_1 \omega}{c} \left[\frac{\omega^2 - \omega_p^2}{(1+\epsilon_1)\omega^2 - \omega_p^2} \right]^{1/2}. \tag{4.27}$$

It is seen in this formula that the dispersion relation has an asymptote for a frequency $\omega_p/\sqrt{1+\epsilon_1}$ (see Fig. 4.5). When plotting this equation, a second branch is obtained for frequencies larger than ω_p. This branch is not a surface wave. Indeed, for $\omega > \omega_p$, the metal dielectric constant is a positive real number so that the metal is a dielectric from the optical point of view. In this regime, the waves can propagate although the refractive index is smaller than 1, indicating that the phase velocity is larger than c. The meaning of this branch of the dispersion relation is clear if one remembers that we did neglect the sign when solving the dispersion relation $\epsilon_1\gamma_2 + \epsilon_2\gamma_1 = 0$.

As ω becomes larger than ω_p, the sign of the dielectric constant changes. In this range of frequency, the Eq. (4.18) is simply the solution of $\epsilon_1\gamma_2 - \epsilon_2\gamma_1 = 0$ or, in other words, the zero of the reflection factor known as the Brewster angle.

Surface Wave on a Lossy Drude Metal. Is it a Surface Plasmon?

In this section, we do not neglect losses. From Eq. (4.18), it is seen that for a real value of the frequency ω, we find a complex value of the wavevector. Alternatively, it is possible to search for a solution of the equation with complex ω and real α. Both possibilities are equally valid. When plotting the real part of ω as a function of the real part of α, we find different dispersion relations as illustrated in Fig. 4.5 depending on the choice. This raises the question of the interpretation of the physical content of each dispersion relation. We shall come back to this subtle issue in Chap. 9.

We now compare the case of low frequencies with the case of optical frequencies. The question that is raised here is the nature of the surface wave for different frequencies. We start by analysing the Drude model in the low- and high-frequency regimes. It is easily seen that we can approximate the dielectric constant by:

$$\begin{aligned} &\omega \gg \gamma(\omega), \quad \epsilon(\omega) \approx 1 - \frac{\omega_p^2}{\omega^2} \\ &\omega \ll \gamma(\omega), \quad \epsilon(\omega) \approx 1 + i\frac{\omega_p^2}{\omega\gamma} = 1 + \frac{i\sigma}{\omega\epsilon_0}, \end{aligned} \tag{4.28}$$

where $\sigma = ne^2/m\gamma$ is the DC conductivity. This form is enlightening as it shows that the optical properties of the metal are dominated by the plasmon response in the optical regime, whereas such properties are dominated by the drag force in the low-frequency regime. In the former case, the dielectric constant is almost a negative real number, whereas in the latter case, it is almost a pure imaginary number. It follows that the plasmonic (oscillatory) character of the surface wave is only meaningful in the regime $\omega \gg \gamma$. Indeed, if we rewrite the equations of motion of the electrons including the friction term as in Eq. (4.2), we find:

$$-\omega^2 x = i\omega\gamma x - \frac{ne^2}{m\epsilon_0}x. \tag{4.29}$$

For large frequencies or small frequencies, we have different approximate expressions:

$$\begin{aligned} &\omega \gg \gamma(\omega), -\omega^2 x + \frac{ne^2}{m\epsilon_0}x = 0 \\ &\omega \ll \gamma(\omega), -i\omega\gamma x + \frac{ne^2}{m\epsilon_0}x = 0. \end{aligned} \tag{4.30}$$

It is clearly seen that the oscillation regime, which is the essence of a plasmon, corresponds only to the case $\omega \gg \gamma$. Instead, for small frequencies, the electronic response of the medium is dominated by the viscous term. Since the typical value of γ is 10^{14} Hz, we note that a surface wave is hardly a surface plasmon for frequencies in the IR or smaller. On the other hand, the plasmonic behaviour (i.e. oscillatory behaviour) dominates the metal response in the case of femtosecond pulses. In summary, whereas from a macroscopic point of view, there is only one well-defined surface wave for any frequency, it turns out that from a microscopic point of view, the underlying behaviour of the electrons is very different in the low- and large-frequency regimes. Beyond this remark on semantics, this distinction is important as the detailed form of the dispersion relation is different for low frequencies and large frequencies as we examine in more detail below.

Dispersion Relation of Surface Waves in the Radio-Frequency Range

Let us analyse in more detail the nature of the surface waves propagating along a conductive surface at low frequencies. We can give a more explicit form of the dispersion relation (4.18) in this regime. At radiofrequencies, the dielectric constant of a metal can be cast in the form: $\epsilon = 1 + \frac{i\sigma}{\omega\epsilon_0} \approx \frac{i\sigma}{\omega\epsilon_0}$ so that the modulus of the dielectric constant is much larger than 1. A Taylor expansion of the wavevector of the surface wave can thus be written in the form:

$$k_{SP} = \frac{\omega}{c}\left[\frac{1}{1+\frac{1}{\epsilon}}\right]^{1/2} \approx \frac{\omega}{c}\left(1+\frac{i\omega\epsilon_0}{2\sigma}\right). \tag{4.31}$$

It is seen that in the limit of the perfect conductor, σ becomes infinite so that the wavevector becomes $k = \omega/c$. This entails that the wave is almost not confined close to the interface. Here, we recover the concept of surface wave used in the context of radio waves propagating along perfectly conducting wires or impinging on perfectly conducting structures. Note in particular that in this limit, there is no more damping as the wavevector becomes real. Let us now check that (4.31) is a valid solution of the equation $\epsilon_1\gamma_2 + \epsilon_2\gamma_1$. In the radio regime, the analysis is very different from the case of the surface plasmon in the optical regime. We consider the case of an interface separating a metal (medium 2) from a vacuum (medium 1) and we use the notation $\epsilon = |\epsilon|\exp(i\phi_\epsilon)$.

$$\begin{aligned}
\gamma_2 &\approx \frac{\omega}{c}[\epsilon]^{1/2} \approx \frac{\omega}{c}|\epsilon|^{1/2}\exp(i\phi_\epsilon/2)\\
\gamma_1 &\approx \frac{\omega}{c}\left[\frac{1}{\epsilon}\right]^{1/2} \approx -\frac{\omega}{c}\left[\frac{1}{|\epsilon|}\right]^{1/2}\exp(-i\phi_\epsilon/2).
\end{aligned} \tag{4.32}$$

The choice of determination of the square root is imposed by the condition $Im(\gamma) > 0$ so that we had to include a sign minus for γ_1. It clearly appears then that the condition $\epsilon\gamma_1 + \gamma_2 = 0$ is satisfied.

To summarize, inserting the Drude model in the dispersion relation of a surface wave yields two limits: the surface plasmon for $\omega > \gamma(\omega)$ and the surface wave with $k = \omega/c$ for $\omega << \gamma$. The latter is the so-called Sommerfeld or Zenneck mode. Note that when dealing with THz waves, the nature of the wave is closer to a radio surface wave than to a surface plasmon.

4.5.3 Electrostatic Limit

In this section, we extend the previous discussion to the non-retarded limit. Let us consider a dipole source oscillating at a frequency $\omega = 2\pi c/\lambda$ at a distance d above the interface such that $d \ll \lambda$. As the distance is much smaller than the wavelength, the interaction between the source and the interface can be described within the electrostatic approximation. Here, we mean that the spatial structure of the field in the near-field of a small object can be computed by solving an electrostatic problem. To justify this statement, it suffices to examine the structure of the field radiated by an oscillating dipole. It is clearly seen that the leading terms are the terms varying as $1/r^3$. These terms yield a time-dependent electric field, which has the *spatial* structure of the field produced by an electrostatic dipole. In other words, the short distance approximation of the Green tensor is the electrostatic Green tensor. It follows that the interface can be modelled by introducing an image charge. The standard electrostatic formalism [16] allows one to introduce an electrostatic reflection factor given by $\frac{\epsilon-1}{\epsilon+1}$. Using a non-lossy Drude model (see next section), this yields a resonance for $\epsilon + 1 = 0$ and hence for $\omega = \omega_p/\sqrt{2}$ in agreement with the qualitative argument given in the first section. This frequency can also be derived by searching a mode of Laplace equation for the scalar potential for a system with one interface separating two homogeneous media [8].

4.6 Surface Phonon Polaritons

4.6.1 Lorentz Model

In the case of a metal and a frequency in the range $[\gamma, \omega_p]$, we have seen that the dielectric constant is negative. In this regime, the surface wave has the character of a surface plasmon. There are other situations such that the dielectric constant becomes negative. In agreement with the Kramers–Kronig relations, they always correspond to frequencies close to resonant excitation of the medium. In the infrared, crystals can absorb light due to the coupling to the optical phonons. There is a frequency range called reststrahlen band where the dielectric constant is negative. A simple

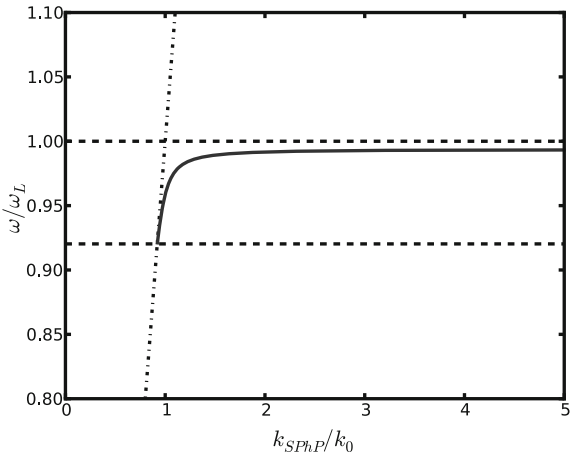

Fig. 4.6 Dispersion relation of a surface phonon polariton propagating along a GaAs/vacuum interface with dielectric constant given by a non-lossy Lorentz model $\epsilon(\omega) = \epsilon_\infty \frac{\omega_L^2-\omega^2}{\omega_T^2-\omega^2}$. The wavevector axis has been normalized by ω_L/c and the frequency axis by ω_L. $\omega_L = 292.1\,\mathrm{cm}^{-1}, \omega_T = 267.8\,\mathrm{cm}^{-1}, \epsilon_\infty = 11$

model allows to show that the dielectric constant can be cast in the form:

$$\epsilon(\omega) = \epsilon_\infty \frac{\omega_L^2 - \omega^2 - i\Gamma\omega}{\omega_T^2 - \omega^2 - i\Gamma\omega} \tag{4.33}$$

where ω_L is the longitudinal frequency and ω_T is the transverse optical frequency. These frequencies are due to the presence of optical phonons. Like for electrons, a longitudinal solution exists at ω_L. It corresponds to a charge density wave. Here, it is a polarization charge density. A detailed discussion can be found in the books by Ziman [13] or Ashcroft and Mermin [12] for example.

There are some differences with the plasmon case. The dielectric constant is negative only in the range $[\omega_T, \omega_L]$. This range corresponds to a wavelength range of the order of 1 μm typically. The central frequency is typically between 10 and 40 μm. Hence, the surface phonon polariton can exist only in the mid-infrared or near THz. A very important similarity of the surface phonon polariton with the surface plasmon is the existence of a horizontal asymptote in the dispersion relation. This indicates the presence of a peak in the local density of states close to the interface as will be discussed later [31, 32]. Figure 4.6 is an example of a dispersion relation of a surface phonon polariton. It corresponds to the case of a wave propagating at the interface between GaAs and a vacuum.

4.7 A Potpourri of Surfaces Waves: Sommerfeld or Zenneck Modes, Quasicylindrical or Lateral Wave

In the previous sections, we have introduced the surface waves as solutions of Maxwell equations in the presence of interfaces. We have seen that there are several cases where a solution can be found for both s- and p-polarizations. Surface waves

often receive different names depending on the frequency range (visible, radio waves) or type of waves (electromagnetics, seismology, acoustics). It turns out that the topic of surface waves is much broader than the topic of surface plasmons. Electromagnetic surface waves have been studied in the context of radiowave propagation well before surface plasmons were discovered. Surface waves have also been studied in different contexts. The purpose of this section is not to give a detailed discussion, but instead to introduce the terminology and to serve as a lecture guide.

4.7.1 Historical Perspective

The concept of surface wave has been introduced by Zenneck at the begining of the nineteenth century. His motivation was to identify the mechanism of long-range propagation of radio waves. The basic idea was that a surface wave decays as $1/r$ instead of $1/r^2$ in 3D. It finally turned out that the correct explanation is the presence of the ionosphere so that the space between the earth and the ionosphere acts as a waveguide. The concept of surface wave was further studied by Sommerfeld when he derived a rigorous solution of the field generated by a dipole above a flat interface separating two homogeneous media. In Sommerfeld's derivation, the surface mode is defined as the contribution of the pole of the reflection factor to the field produced by a dipole above an interface. This definition agrees with our remark on the previous section linking the surface wave with the pole of the reflection factor. This surface wave is often named after Zenneck or Sommerfeld. The much debated existence of a surface wave in the radio literature is due to the fact that the field has a complex structure. It should be stressed that there is perfect consensus on the integral form of the field radiated by a dipole above an interface. Yet, such an integral is not useful for practical applications. Several authors have therefore derived approximate analytical expressions valid in different cases. It is only when it comes to the interpretation of the different contributions that there is a debate. The reader will find a detailed account of these works in the books by Brekhovskikh [1], Banos [2], Felsen [3], King [4] and a recent review paper by Collin [34]. To make a long story short, let us summarize the situation as follows. The field radiated by a dipole can be decomposed into a sum of plane waves. In the presence of an interface, each plane wave is transmitted and reflected. The total field is hence the field radiated by the source plus a sum of plane waves weighted by the corresponding Fresnel factors. When performing the integral over all reflected plane waves, one can extract the pole contribution due to the pole of the reflection factors. This contribution yields the surface waves. There is a second contribution that appears when using analytical techniques to evaluate asymptotically the integral in the complex plane: it is the contribution along the branch cuts in the complex plane. We give a very brief account of this wave in the following section.

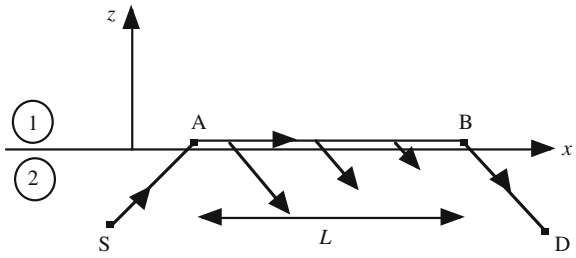

Fig. 4.7 Illustration of the lateral wave. The wave propagates from the source to the interface at the critical angle. After refraction, it propagates along the interface as a plane wave and reenters the medium continuously. This contribution becomes dominant when the medium is lossy so that direct propagation in the medium is rapidly damped

Lateral Wave

The second noteworthy contribution is called lateral wave in the radiowave and seismology community. It has been investigated only recently [35] in the optics community and was called quasicylindrical wave [36, 38] or Norton wave [39]. An extensive discussion of this wave in the context of propagation of radio waves along the earth was written by King [4]. In this section, we briefly describe a physical picture of the origin of the lateral wave. Let us consider a source located at $z = -d$ in a material medium with refractive index n. The lateral wave is the wave corresponding to propagation from the source to the interface at the critical angle followed by a refraction at the interface and propagation by a plane wave parallel to the interface in the medium $z > 0$ (see Fig. 4.7). When the medium at $z < 0$ is absorbing and the medium $z > 0$ is not absorbing, this is the most efficient mechanism for propagation over large distances as most of the energy is in the nonabsorbing medium. When excited by a line, this two-dimensional wave decays as $1/L^{3/2}$ where L is the distance of propagation along the interface. Instead, the surface wave has an exponential decay.

The lateral wave is very well known in seismology. An excellent account of surface waves in elastic media can be found in the textbook by Aki and Richards [40]. In the context of radiowaves, it has received a lot of attention in the 1960s and 1970s. The reader will find a detailed account in the works quoted above [1–4, 34]. Of particular interest in optics are Refs. [35, 36, 38, 39] where it has been shown that these waves cannot be neglected in many cases when studying propagation and scattering along metallic surfaces including the resonant transmission phenomenon [37].

In what follows, we focus on key properties of surface plasmons related to (i) the local density of states, (ii) the spatial confinment and (iii) the fast temporal response. Regarding these three aspects, surface plasmons are very different from lateral waves. These properties are intimately linked to the underlying electronic character of the surface plasmon polariton.

4.8 Key Properties of SPP

Plasmonics has become a very active area of research due the large number of applications. However, all these applications rely on a small number of key properties. The purpose of this chapter is to discuss these key properties of surface plasmons in simple and general terms. We will first analyse the importance of having a dispersion relation with very large wavevectors. We will discuss the implications in terms of field confinment and the implications in terms of local density of states. Finally, we will discuss the spectral width of surface plasmon excitation and its significance in terms of ultrafast response.

4.8.1 Confinment of the Field

A large number of applications of surface plasmons rely on the possibility of producing highly confined fields and/or to produce or observe light at a length scale smaller than the wavelength in a vacuum. The purpose of this section is to review the basic properties of surface plasmons underlying these applications. Let us first consider the case of surface plasmons propagating along flat interfaces. It is necessary to distinguish between confinment of the field along the normal of the interface and confinment in the plane of the interface. We have already given some orders of magnitude of the field confinment away from the interface in Table 4.1. We now discuss the potential of surface waves for in-plane confinment.

Lateral Confinment

The losses introduce a limitation to the extent of the surface waves along the interface. The decay length is given by $1/Im(k_{SP})$. This value depends significantly on the losses of the material. A typical order of magnitude for noble metals and visible frequencies is a few micrometers. We note that this length is considerably reduced for frequencies close to the asymptote of the dispersion relation. The main reason is connected to our previous discussion. A photon-like surface plasmon is poorly localized close to the interface and has most of its energy in the dielectric above the metal where there are no losses. By contrast, a plasmon-like surface plasmon has a large part of its energy in the metal so that it is very sensitive to the losses. It is a general rule that modes with most of the field energy in the dielectric have a longer propagation length. In practice, another mechanism can reduce the propagation length. It is due to radiative leakage of energy (often called radiative losses) due either to scattering by random roughness or by diffraction by a periodic structure such as a grating.

We have discussed the larger length scale of a surface plasmon along the interface. We now address the issue of the smallest length scale. Let us remind what is the

origin of the confinment limit in a vacuum when dealing with a monochromatic field at frequency ω. Due to the dispersion relation in a vacuum, the wavector modulus is given by $k = \omega/c$. Let us assume that we consider an electromagnetic field in the vacuum far from any boundary. The field can then be decomposed into a sum of planes waves with real wavectors. A property of Fourier transform gives $\Delta x \Delta\alpha \geq 2\pi$ where α is the x-component of the wavector. If we deal with a field in a vacuum far from any surface or object, the modulus of the wavevector is given by ω/c so that the smallest possible size of the field along the x-axis is given by $2\pi/\alpha_{max} = \lambda$. Hence, the field cannot vary rapidly as it would, close to a tip for example.

By contrast, it was seen in Fig. 4.5b that the maximum wavector given by the plasmon dispersion relation may be much larger than ω/c. This seems to pave the way to a strong confinment of the field. There have been some attempts to take advantage of this strong localization of the field. It has been proposed by Pendry that this property can be used to realize a superlens [41] with a simple thin film supporting surface plasmons. The experimental implementation has been reported by two groups in the visible using silver [42] and in the infrared using SiC [43]. Another proposal for superresolution based on the use of surface plasmons was put forward in Ref. [44]. The key idea was to take advantage of the large wavevectors that are seen on the dispersion relation (with the choice of a real wavevector and a complex frequency). A debate followed that proposal [45, 46]. However, in practice, it is not possible to fully take advantage of this property of surface plasmons because losses play an important role. We shall show in Sect. 4.9 that the relevant dispersion relation that must be used for discussing confinment of the field is the dispersion relation shown in Fig. 4.5a. It is seen that the wavector modulus is limited due to the so-called backbending of the dispersion relation. This entails that the surface plasmons always have an intrinsic limitation in terms of resolution. This is a rather severe limitation as in many cases, the maximum value of the wavector is hardly larger than $2\omega/c$. Let us stress that so far, the resolution obtained in different experimental results [42, 43] appears to be indeed limited by the losses.

However, surface plasmons are often used to produce highly localized spots that go well beyond these limitations. In all the practical examples, the origin of the localization of the fields lies in the spatial structure of the material. In most cases, one uses nanometric particles or nanostructures such as nanowires, nanoholes or indentations in a metallic substrate. Examples include the first implementation of near-field optical microscopes [47, 48], the strong confinment obtained using nanoholes [49] and the use of tips as nanosources [50, 51]. One might then ask what is the role of plasmons in that case? A simple answer can be obtained by analysing the fields produced by a subwavelength spherical particle of dielectric constant ϵ and radius a (see the chapter by J. Aizpurua). If $a \ll \lambda$, the non-retarded approximation is valid so that the spatial structure of the field can be found using an electrostatic approximation. The scattered field is given by the field of a dipole for a distance $r > a$. The field decays as $1/r^3$ for $r > a$ so that the confinment is only limited by a. This confinment is due to the geometry and not to the plasmon, it is independent of the material properties. Yet, the amplitude of the field depends on the material properties at the particular frequency considered. For instance, when dealing with a

spherical nanoparticle with radius a, its polarizability α_p can be written as:

$$\alpha_p = 4\pi a^3 \frac{\epsilon(\omega) - 1}{\epsilon(\omega) + 2}. \tag{4.34}$$

In the previous equation, it is clearly seen that the only limitation to the confinment is the fact that the amplitude of the dipole tends to zero with a. However, if the frequency is such that $\epsilon(\omega) + 2$ is almost zero, a resonance is excited as it will be discussed in more detail in Sect. 4.8.3. Within the Drude model, this condition is satisfied for $\omega = \omega_p/\sqrt{3}$. Thus, it is seen that a surface plasmon resonance of a particle is useful for light confinment indirectly: its role is to compensate for the small value of the dipole moment of a small object.

In the above example, we have seen that the form of the electric field close to a particle can be factorized in two terms. The dependence on space variables is the electrostatic form of the dipolar field, the frequency dependence is given by the polarizability. Only the latter has a resonant behaviour which is the signature of the plasmon resonance.

This concept of confinment by geometry coupled to resonance enhancement has been put forward by Li, Stockman and Bergman who proposed to use a chain of nanoparticles to realize an efficient nanolens [52].

Finally, we mention another possibility for confining the field. Metal/dielectric/metal (MDM) structures can support surface modes which are plasmonic even if the dielectric is only a few nanometers thick so that these modes are highly localized in the gap [53]. Remarkable guiding properties have been demonstrated using channel surface polaritons which essentially rely on this type of structure [54]. Other applications of the confinment in MDM structures include applications for light emission in the weak coupling regime [55] and achieving strong light-matter coupling [56]. These are intimately related to the concept of local density of states that we now introduce.

4.8.2 Surface Plasmons Contribution to the Local Density of States

The lifetime of an atom can typically be reduced by orders of magnitude when it is located close to an interface. This has been first demonstrated experimentally by Drexhage [57]. Excellent discussions can be found in Refs. [17, 58, 59]. Similarly, the electromagnetic energy density at thermodynamic equilibrium can be increased by orders of magnitude close to an interface [31, 60]. Both phenomena depend on the density of electromagnetic states. The changes by orders of magnitude are the clear signature of a change of the physical phenomena that determine the local density of states. In both cases, the contribution of surface waves plays a key role. The purpose of this section is to briefly review the concept of Local Density Of States (LDOS)

and to show how the surface waves may drastically modify it. We will briefly discuss applications to light emission assisted by surface waves. We will also show that the influence of surface plasmons on the LDOS plays a key role in the Casimir force, a pure quantum electrodynamics phenomenon.

Elementary Introduction to the Density of Electromagnetic States

Before starting the discussion, we make a remark on semantics regarding the meaning of state, mode and eigenfunction. The word "state" is usually used in the context of quantum mechanics or statistical physics, whereas the word "mode" is often used in the context of wave theory. Both words deal with eigenfunctions of linear operators so that the terms are often interchanged. The term density of states is used for $g(\omega)$ such that $g(\omega)\mathrm{d}\omega$ is the number of states (modes) with frequency in the interval $[\omega, \omega + \mathrm{d}\omega]$. To begin, we briefly remind how to derive the density of electromagnetic states or, in other words, how to count the number of different solutions (plane waves) of Maxwell equations in a vacuum. We will then analyse how the presence of surface waves modifies the situation. It is useful to introduce a virtual cubic box of size L and to look for fields satisfying periodic boundary conditions. Indeed, this allows one to discretize the solutions and therefore to count them. From the periodic boundary condition, it follows that the wavevector components are of the form $\alpha = n2\pi/L, \beta = m2\pi/L, \gamma = l2\pi/L$ where n, m, l are integers. In k-space, the volume occupied by a state is therefore $(2\pi/L)^3$ so that the number of states in the volume element $\mathrm{d}\alpha\mathrm{d}\beta\mathrm{d}\gamma$ is $2L^3\mathrm{d}\alpha\mathrm{d}\beta\mathrm{d}\gamma/(2\pi)^3$ where the factor 2 accounts for the two possible polarizations of each state. The density of states in k-space per unit volume is thus given by $1/4\pi^3$. We can now easily find the number of states with a given frequency $\omega = ck$. They occupy the volume $4\pi k^2\mathrm{d}k$ in k-space. Using the dispersion relation $k = \omega/c$, we find the number of states per unit volume in the range $\omega, \omega + d\omega$:

$$g_v(\omega)\mathrm{d}\omega = \frac{\omega^2}{\pi^2 c^3}\mathrm{d}\omega, \tag{4.35}$$

where we have introduced the density of states per unit volume $g_v(\omega)$ in a vacuum. We now illustrate the importance of this concept using three examples. Let us first count how many states $N(\omega)$ are available between 0 and ω in a volume V:

$$N(\omega) = V\int_0^{\omega} g_v(\omega')d\omega' = V\frac{\omega^3}{3\pi^2c^3} = \frac{8\pi}{3}\frac{V}{\lambda^3}. \tag{4.36}$$

The simple rule to remember is that the number of states with frequency smaller than ω is roughly given by the volume divided by $(\lambda/2)^3$. The second example is the form of the energy of the blackbody radiation. Each mode has a quantum of energy $\hbar\omega$ and the mean excitation number is given by Bose–Einstein statistics

$n_{BE}(\omega) = 1/[\exp(\hbar\omega/k_B T) - 1]$. The product of these two terms by the density of states yields the Blackbody density of energy at temperature T:

$$u(\omega, T) = \frac{\hbar\omega^3}{\pi^2 c^3} \frac{1}{\exp(\hbar\omega/k_B T) - 1}. \tag{4.37}$$

We now show how the local density of states plays a key role in the lifetime of a two-level system. From the Fermi golden rule, it is known that the lifetime is proportional to the number of final states. When studying the rate of radiative relaxation, the radiative decay rate is therefore proportional to the number of electromagnetic states at the corresponding frequency. This can be seen by comparing the stimulated and spontaneous emission rates given by the Einstein coefficients. Their ratio is given by:

$$\frac{A_{21}}{B_{21}\hbar\omega} = \frac{\omega^2}{\pi^2 c^3}, \tag{4.38}$$

which is nothing but the vacuum density of states. For stimulated emission, only the mode of the incident photon has to be considered, whereas for spontaneous emission, one has to sum over all possible electromagnetic states. Hence, the spontaneous emission coefficient is proportional to the LDOS. Let us finally point out a slight difference in the definition of local density of states depending on the application: evaluating the equilibrium energy or evaluating spontaneous emission. A two-level system that is coupled to the electromagnetic field through an electric dipole moment can couple only to the component of the electric field parallel to the electric dipole. The relevant form of the local density of states is thus called projected-LDOS as only one component of the field matters. In a vacuum, this is simply a factor 3 difference as the field is isotropic. In more complex situations, the LDOS can be different for different polarizations. It is well known for instance that the lifetime of a molecule close to an interface depends on the orientation of its dipole moment.

To summarize, the concept of density of states plays a key role when looking at the radiative decay of a two-level system and when looking at the thermodynamic properties of electromagnetic radiation. In what follows, we shall analyse how the presence of surface plasmons drastically modifies the density of states. We will give a hint of the physical reason behind this phenomenon and derive from it an upper limit of the number of states.

Electron and Phonon Density of States

We have pointed out that surface plasmons are polaritons. In other words, they are half photons, half electrons. Since electrons are also described by waves, the same technique can be used to analyse the density of states. The density of states in k-space is also given by $1/4\pi^3$ for electrons. Here, we have accounted for the degeneracy due to the spin $1/2$ of the electron. The total number of states in a crystal of volume V with N atoms is given by $2N$ for a s band. Similarly, the total number of phonon

states is given by $3N$ because this is simply the total number of degrees of freedom of the atoms. Hence, the number of states per unit volume is roughly N/V, which is the inverse of the volume a^3 of a unit cell of the crystal. If we now compare the number of states available for light in a vacuum ($(2/\lambda)^3 \approx 10\text{–}19\text{m}^{-3}$) and for condensed matter excitations ($1/a^3 \approx 10\text{–}30\text{m}^{-3}$), we find a difference of 11 orders of magnitude.

This crude estimate shows what is the key to the efficiency of plasmons or optical phonons in increasing the energy density or in reducing the lifetime of quantum emitters. The density of states of polaritons benefits from the large number of states of condensed matter excitations (electrons or phonons). However, many of these modes do not contribute to surface waves. A better estimate of the number of surface plasmons can be obtained by working with the dispersion relation and introducing a cut-off at ω/v_F as we will discuss below.

Increasing the Density of States: Surface Waves, Slow Light and Microcavities

Let us make a pause in the discussion of surface wave density of states and make a comment regarding the increased density of states in a waveguide with slow velocity. It is known that slow velocity systems can be used to increase the density of states. The mechanism is depicted in Fig. 4.8. As the dispersion relation becomes flat close to the band edge, the number of states (represented by dots) with a frequency in the interval $\Delta\omega$ increases. This behaviour is known as van Hove singularity. A major advantage of photonic crystals is that there are almost no losses in dielectric media. Since the density of states diverges (the group velocity becomes zero), these systems seem to be the perfect solution to engineer the optical properties of quantum emitters. Yet, it is important to emphasize that the number of states available when using a waveguide is always finite. A plasmonic system can provide a local density of states which is orders of magnitude larger than what can be achieved with a slow waveguide. In order to understand this apparent paradox, let us first remind about the derivation of the density of states for a one-dimensional system. We consider a waveguide branch characterized by a dispersion relation $k_z(\omega)$ for a mode propagating along the z-axis in a periodic waveguide with period a. In order to count the number of modes, we again consider that the system has a finite length L and we introduce the so-called Born von Karman (or periodic) boundary conditions stipulating that the system is periodic with period L along z. It follows that $k_z = p\,2\pi/L$. The number of modes in the interval $\mathrm{d}\omega$ corresponding to an interval $\mathrm{d}k_z$ is given by

$$g(\omega)\mathrm{d}\omega = \frac{L}{2\pi}\mathrm{d}k_z = \frac{L}{2\pi}\frac{\mathrm{d}k_z}{\mathrm{d}\omega}\mathrm{d}\omega. \tag{4.39}$$

It is seen that the density of states diverges as the group velocity goes to zero. However, one should keep in mind that *this divergence is integrable* so that the number of states in a finite interval $[\omega_1, \omega_2]$ always remains finite.

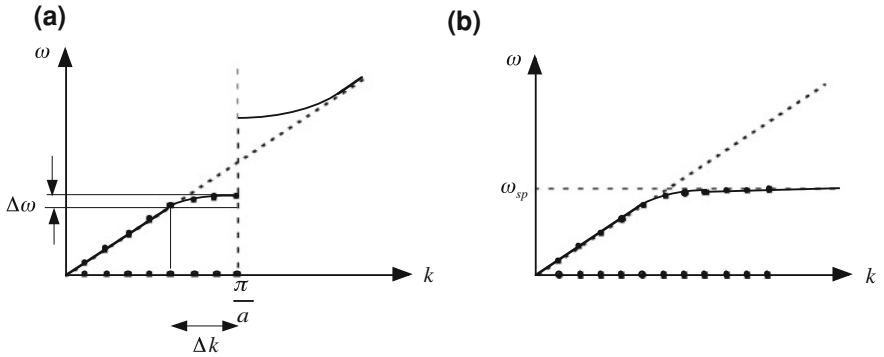

Fig. 4.8 Increasing the density of states. States are characterized by k and ω. They correspond to a point located on the dispersion relation. In k-space, the density of states per unit length is constant and takes the value $1/2\pi$. **a** shows that in ω space, the density of states increases close to the gap edge, **b** shows that the increase close to the asymptote is considerably larger as the asymptote is not limited along the k-axis

This is clearly seen in Fig. 4.8 where we represent schematically the dispersion relation of a guided wave close to a band edge and the dispersion relation of a surface plasmon. It is seen that the modes are simply redistributed close to the band edge so that this only concerns a finite number of modes although mathematically the density of states diverges. An upper value of the number of modes involved is clearly the size of the Brillouin zone $2\pi/a$ divided by the interval between two modes $2\pi/L$. We find L/a. The period of a photonic crystal is of the order of the wavelength so that we obtain an estimate of an upper bound of the number of modes in a photonic crystal given by L/λ. This is orders of magnitude less than the number of modes available with surface waves at resonance.

We now discuss briefly another possibility for increasing the density of states originally proposed by Purcell. The idea is to use a cavity with a single mode. The number of states per unit volume is thus $1/V$ where V is the cavity volume. Taking into account the finite value of the quality factor of the cavity, we obtain for a Lorentzian resonance a density of states:

$$g(\omega) = \frac{1}{V}\frac{\gamma}{2\pi}\frac{1}{(\omega-\omega_0)^2+\gamma^2/4}. \tag{4.40}$$

At resonance, the density of states is thus given by:

$$g(\omega_0) = \frac{2}{\pi V\gamma}. \tag{4.41}$$

The Purcell factor is the local density of states in the cavity normalized by the density of states in a vacuum[1]:

$$F_p = \frac{2}{\pi V \gamma} \frac{3\pi^2 c^3}{\omega^2} = \frac{3}{4\pi^2} Q \frac{\lambda^3}{V}, \tag{4.42}$$

where $Q = \omega_0/\gamma$. This derivation is based on a poorly defined volume. A more accurate description should account for the polarization of the mode field as well as its space dependence. Indeed, the field in a cavity is not uniform so that the coupling between a mode and an emitter will strongly depend on the exact location of the emitter. A more detailed analysis can be found in Refs. [66–68].

Local Density of States Due to Surface Waves

We first start the discussion of the role of surface waves on the local density of states with a qualitative discussion based on the dispersion relation. We then present a more quantitative analysis. It is seen in Fig. 4.8 that the number of states provided by a surface plasmon at resonance is infinite as the dispersion relation seems flat and unbounded. This is not correct and is a consequence of the model of the dielectric constant that does not account for the non-locality. A non-local dielectric constant introduces a cut-off [17] in the dispersion relation given by $v_F \omega_{SP}/\sqrt{2}$ where v_F is the Fermi velocity as already discussed. We can now easily compare the density of states due to surface plasmons to the vacuum density of states. A rough estimate of the number of surface plasmons per unit area is given by dividing the area of a disk with a radius $\pi k_{SP,\max}^2$ by the area per state $1/4\pi^2$:

$$\frac{\pi k_{SP,\max}^2}{4\pi^2} \approx \frac{\omega_{SP}^2}{4\pi v_F^2}, \tag{4.43}$$

which is clearly much larger than what we found for dielectrics where the order of magnitude is $1/\lambda^2 \approx \omega^2/c^2$. We remind that c/v_F is typically on the order of 300.

We now turn to a quantitative analysis of the local density of states due to surface waves. An explicit form can be derived from the imaginary part of the Green tensor. The reader will find a detailed analysis in Ref. [32]. Of particular interest is the asymptotic expression of the local density of states at a distance z from the interface such that $z \ll \lambda$.

$$\frac{g(z,\omega)}{g_v(\omega)} = \frac{Im[\epsilon]}{|\epsilon+1|^2} \frac{1}{4(k_0 z)^3}, \tag{4.44}$$

where $g_v(\omega)$ stands for the vacuum density of states. The surface plasmon resonant contribution is clearly given by the term $1/|\epsilon+1|^2$. Figure 4.9 illustrates the contri-

[1] In the context of Fermi golden rule, a factor 1/3 is introduced in order to account for the fact that a given dipole can couple to only one component of the electric field.

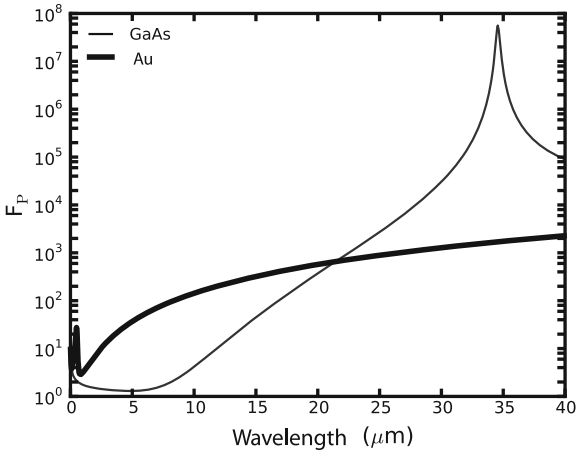

Fig. 4.9 Local density of states at a distance of 10 nm above an interface separating a vacuum from gold or GaAs

bution of this term to the LDOS at a distance of 10 nm of a gold surface and a GaAs surface.

In both cases, the presence of the surface wave results in a peak in the LDOS. It clearly appears that the role of the surface phonon polariton is orders of magnitude more important than the surface plasmon.

Local Density of States and Energy Transfer at Nanoscale

Another remarkable consequence of the increase of the density of states due to surface waves is the increase of energy density at equilibrium. Since the modes are thermally excited at equilibrium, there is a large energy density close to the interface. Figure 4.10 illustrates the evolution of the energy spectral density at different distances from an interface separating SiC from a vacuum. Two features appear clearly in this figure: (i) the energy density normalized by the energy density of a blackbody is increased by several orders of magnitude and (ii) the spectrum becomes quasimonochromatic. The existence of surface waves thermally excited has been observed experimentally by de Wilde et al. [61] who were able to obtain near-field images of samples without external illumination. We note that in the near-field, the spectrum becomes quasimonochromatic indicating that the field is partially temporally coherent. The coherence time is essentially the decay time of the surface phonon polariton as discussed in Refs. [31, 33].

As a consequence of this increase of energy density close to the interface, the heat transfer between two half-spaces separated by a distance smaller than the wavelength increases. This heat transfer mechanism can be viewed as mediated by the surface phonon polaritons. Since the number of surface waves increases dramatically at small distance, the heat flux through a vacuum gap can be enhanced by orders of magnitude. This effect due to surface waves was predicted in Refs. [62, 63] and measured recently

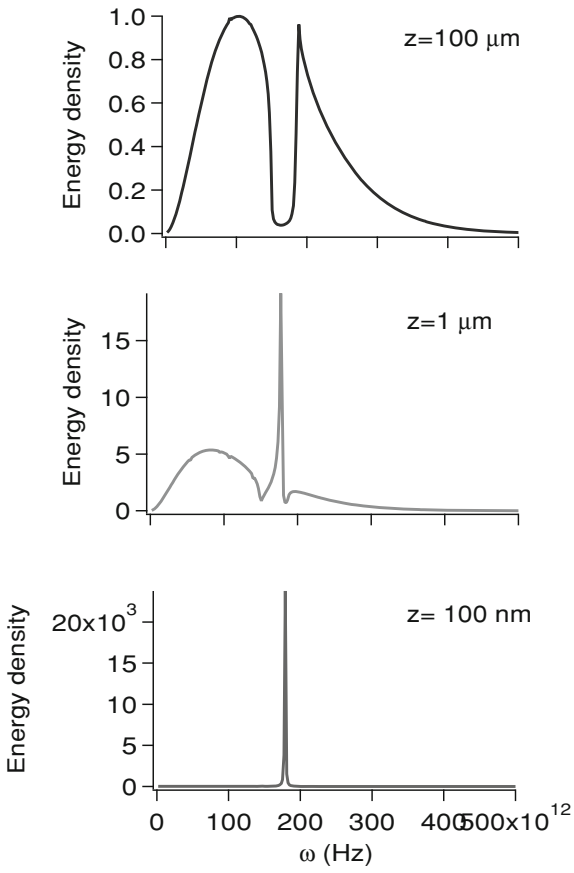

Fig. 4.10 Electromagnetic energy density at equilibrium at 300 K as a function of distance from an interface vacuum/SiC. The energy density is normalized by the maximum blackbody value at 300 K

[64, 60]. The heat transfer through the gap due to this surface phonon interaction can be viewed as a phonon tunelling phenomenon. It can also be described in a form similar to the Landauer conductance. It has been shown recently [65] that each mode characterized by (α, β, ω) yields a contribution to the radiative heat conductance proportional to the thermal quantum of conductance $\pi^2 k_B^2 T/3h$ and a transmission factor where k_B is Boltzmann's constant and h is Planck's constant.

Local Density of States and Light Emission Assisted by Surface Waves

In the introduction of this section, we have cited the pioneering experiment by Drexhage showing that the lifetime of an emitter can be drastically reduced close to an interface. When the distance is below 5 nm, the energy goes into heat in the substrate and surface plasmons do not provide a significant contribution to this mechanism.

However, if the distance is larger than approximately 10 nm, most of the energy goes into the surface plasmon for appropriate frequencies. In the case of a flat surface, this energy is then converted into heat. However, if e.g. a grating is ruled on the surface, the energy can be radiated. In that case, the surface works as an antenna: the energy of the source is efficiently coupled into the surface (due to the large LDOS) and then efficiently radiated by the surface (due to the grating). This idea has been put forward in the context of light-emitting diodes [69, 70]. The influence of the surface plasmon resonance on the single molecule fluorescence assisted by a resonant particle has been investigated theoretically [71, 72]. Quantum wells' light emission assisted by surface plasmons has been demonstrated more recently [73]. A remarkable demonstration of optical nanoantennas at the level of a single emitter has been reported using metallic nanospheres. An emitter located at a distance of the order of 10 nm excites efficiently the surface plasmon of the particle. By properly choosing the radius of the particle, it is possible to increase the ratio of power emitted versus the power absorbed in the particle so that the nanosphere becomes an efficient nanoantenna. Two experiments have clearly demonstrated how metallic nanospheres can be used as efficient nanoantennas to increase molecules' fluorescence [74, 75]. More recently, several metallic structures have been proposed as antennas to control the angular emission and also increase the emission rate [55, 76, 77].

Local Density of States and Casimir Force

Another consequence of the contribution of surface plasmon to the LDOS is the Casimir force between two metallic parallel plates. Casimir force is a pure quantum electrodynamics effect that manifests itself at macroscopic scale. Casimir predicted [78] that there is an attractive force between two parallel perfectly conducting surfaces at 0 K separated by a gap of width d. Since then, his remarkable prediction has been measured experimentally with great accuracy [79–81]. However, when comparing the measurements with the data, the assumption of a perfect conducor cannot be used any longer [82]. A careful analysis shows that the surface plasmons are responsible for the forces actually observed [83–85]. We give here a brief qualitative discussion of this effect. We refer the reader to references [83] for a further discussion. The gap behaves as a waveguide with a set of modes. From the quantum electrodynamics point of view, each mode (k, ω) has a zero point energy at 0 K given by $\hbar\omega$. It follows that the total energy is given by $\sum_n \hbar\omega_n$ where the sum is over all modes of the gap. Since the number of modes in the gap decreases when the width d decreases, the energy also decreases. Hence, the electromagnetic energy plays the role of an attractive potential. In the original derivation of Casimir, modes of a planar waveguide with perfectly conducting surfaces were used. When accounting properly for the optical properties of metals, it turns out that the density of states is dominated by the surface plasmon contribution.

4.8.3 Broad Spectrum and Fast Response

When comparing plasmonic resonators with dielectric resonators, the presence of losses in the metal is often put forward. The quality factor of the resonator depends on the dielectric constant of the material. To illustrate this idea, we consider the polarizability of a small sphere. Close to the sphere resonance, we can expand the dielectric constant. We use the notation $\epsilon(\omega) = \epsilon_R(\omega) + i\epsilon_I(\omega)$ and assume that $\epsilon_R(\omega_0) = -2$.

$$\begin{aligned}\epsilon(\omega) &\approx \epsilon_R(\omega_0) + \frac{\mathrm{d}\epsilon_R}{\mathrm{d}\omega}(\omega - \omega_0) + i\epsilon_I(\omega_0) \\ &\approx -2 + \left(\frac{\mathrm{d}\epsilon_R}{\mathrm{d}\omega}\right)_{\omega_0}[\omega - \omega_0 + i\Gamma],\end{aligned} \tag{4.45}$$

where $\Gamma = \epsilon_I(\omega_0)/[\mathrm{d}\epsilon_R/\mathrm{d}\omega]$. The polarizability can be approximated by a Lorentzian profile:

$$\alpha(\omega) = 4\pi a^3 \frac{\epsilon(\omega) - 1}{\epsilon(\omega) + 2} \approx \frac{12\pi a^3}{\left(\frac{\mathrm{d}\epsilon_R}{\mathrm{d}\omega}\right)} \frac{1 - i\epsilon_I(\omega_0)/3}{\omega_0 - \omega - i\Gamma} \tag{4.46}$$

We have already seen that metallic losses in the optical frequency regime are due to electron–electron interaction and to electron–phonon interaction. These processes have a low dependence on temperature so that they cannot be suppressed. Hence, these losses are a specific property of a plasmonic resonator. They result in two properties of surface plasmons. The quality factor of the resonance depends on the imaginary part of the dielectric constant at the resonance frequency. A typical quality factor for plasmons is between 10 and 100. Accordingly, the relaxation time of the system in the visible is of the order of a few femtoseconds. A small quality factor can be viewed as a drawback in terms of Purcell effect for instance. On the other hand, a resonator with a large bandwidth can be very interesting. In particular, it allows one to perform a coherent control of pulses on extremely short time scales. This particular property is the basis of a large number of recent contributions [86, 87]. Another important application is the possibility of designing a nanoantenna with a broad bandwidth [55].

Finally, we should emphasize that the relaxation time of a plasmonic resonance does also depend on the geometry of the structure. To illustrate this idea, we discuss the example of the so-called long-range and short-range surface plasmons on symmetric thin metallic films in a dielectric first investigated by Sarid [88]. In order to understand why the geometry influences the relaxation time of a plasmonic mode, it is sufficient to realize that the field of the long-range surface plasmon energy is mostly in the non-lossy dielectric, whereas the short-range surface plasmon is more confined in the metal where losses take place. This has also been widely discussed in the context of shell structures [89]. In both cases, the coupling between two modes

depends on the thickness of the metal film and allows to control the resonance frequencies.

4.9 Surface Plasmon Polaritons on Lossy Materials

As already mentionned, the dispersion relation given by (4.18) cannot be solved by using a real frequency and a real wavevector when the dielectric constant is complex. Yet, a solution can be found when using either a complex α and a real ω or vice versa. These two choices lead to different shapes of the dispersion relation as seen in Fig. 4.5. One dispersion relation has an asymptote for very large values of α, while the other has limited values of α and presents a backbending. We have discussed the key properties of surface plasmon with emphasis on the lateral confinment (e.g. necessary for a super lens) and on the large LDOS (e.g. necessary for nanoantennas). Since the existence of a horizontal asymptote plays a key role both for the transverse confinment of the field (large k values of surface plasmons are needed) and for the LDOS (flat dispersion curve), it is important to establish a prescription on which choice should be made when looking for a dispersion relation. In this section, we discuss the origin and physical content of these two dispersion relations summarizing Ref. [90] where further details can be found.

4.9.1 First Interpretation

The existence of two different forms of the dispersion relation was first pointed out by Alexander [91]. It was first thought that the dispersion relation with a backbending was an unphysical mathematical curiosity. Yet, Arakawa [92] remarked that when plotting the position of the dips in a reflectivity experiment where the angle of incidence is varied at fixed frequency, the dispersion relation presents a backbending branch. Instead, when plotting the points obtained from a spectrum at fixed angle, one finds the dispersion relation without backbending. This approach gives a practical prescription for the analysis of attenuated total reflection (ATR) experiments. We can go beyond this simple observation and note that when measuring a reflectivity spectrum at fixed angle, the experiment contains the following ingredients: a real incident wavevector, a reflectivity spectrum showing a resonance at a given (real) frequency with a width that accounts for the imaginary part of the frequency. Similarly, a reflectivity measurement done at fixed frequency for different angles displays a resonance peak at a given (real) wavevector with a width that accounts for the imaginary part of the wavevector.

Nevertheless, this discussion is not a general prescription that can be used to discuss all possible issues. To illustrate this point, we consider two questions regarding important properties of surface plasmons: confinment of the fields and large density of states. What can we learn from the dispersion relation regarding these questions?

The dispersion relation with a backbending predicts a cut-off spatial frequency k_{co}: it follows that the LDOS has an upper bound and that the maximum confinment of the field is also limited by $1/k_{co}$. By contrast, the dispersion relation without backbending predicts a divergence of the LDOS at the frequency corresponding to the asymptote of the dispersion relation. It also predicts no limit to the possible resolution. It is thus clear that a general discussion on the applicability of the different dispersion relations is needed.

4.9.2 Representation of the Fields

In order to analyse the meaning of the dispersion relation and to clarify this issue, it is necessary to investigate the meaning of the choice of a real or complex wavevector. In what follows, we emphasize that the relevant quantity is not a field with real or complex wavevector, but the field which depends on time and position. Introducing complex or real wavevectors amounts to introduce a particular representation of the field. A standard and convenient representation is the Fourier transform of the field with respect to both time and position. The resulting modes have real frequencies and real wavevectors. We note that a Fourier transform can always be introduced for a square integrable function in time and space. Any field that carries a finite energy is square integrable in time and space so that we can use a Fourier representation.

When looking at the field excited by any distribution of sources in the presence of an interface, it is possible to extract the pole contribution to the integral. Following Sommerfeld's prescription, this contribution of the pole of the Fresnel reflection or transmission factor to the integral is the surface wave. The contribution of the pole can be evaluated analytically using the residue theorem. This first analytic integration can be done either over frequencies or over the wavevector. Since the pole is complex, the analytic integration yields either a complex wavevector or a complex frequency depending on the choice. When following this program, we find two different representations of the surface plasmon field equally valid since the final value of the integral does not depend on the way chosen to perform the evaluation. One representation uses surface modes with real frequency and complex wavevector, whereas the other uses complex frequencies and real wavevectors. We skip all details and give the result of the integration reported in Ref. [90] hereafter.

Field Representation with a Real Wavevector

The field can be cast in the form of a linear superposition of modes with real wavevector $\mathbf{K}$ and complex frequency ω_{SP}. We denote $\mathbf{K}$ the projection of the wavevector parallel to the interface $\mathbf{K} = (\alpha, \beta, 0)$:

$$\mathbf{E}_{SP} = 2\Re\left[\int \frac{\mathrm{d}^2\mathbf{K}}{(2\pi)^2}\, E(\mathbf{K}, t)\left(\hat{\mathbf{K}} - \frac{K}{\gamma_m}\mathbf{n}_m\right) e^{i(\mathbf{K}\cdot\mathbf{r}+\gamma_m|z|-\omega_{SP}t)}\right], \tag{4.47}$$

where $\mathbf{n}_m = -\hat{\mathbf{z}}$ if $z < 0$ and $\hat{\mathbf{z}}$ if $z > 0$, and $\hat{\mathbf{K}} = \mathbf{K}/K$. The surface plasmon field takes a form that looks as a mode superposition, *except that the amplitude* $E(\mathbf{K}, t)$ depends on the time t. Indeed, when describing a stationary field using modes that have an exponential decay, the amplitude is necessarily time dependent. In order to obtain a superposition of modes with fixed amplitudes, it is necessary to assume that all sources are extinguished after time $t = 0$ so that we observe the field after it has been excited. In that case, the decay of the mode is well described by the imaginary part of ω_{SP}. Equation (4.47) is thus well suited for fields excited by pulses. Note that the polarization of each mode is specified by the complex vector $\hat{\mathbf{K}} - \frac{K}{\gamma_m}\mathbf{n}_m$, whose component along the z-axis depends on the medium from which the field is evaluated.

Field Representation with a Real Frequency

A different representation of the field can be derived using modes characterized by a real frequency ω and a real β. The x-component of the wavector is complex and is given by

$$K_{x,SP} = [k_{SP}^2 - \beta^2]^{1/2}. \tag{4.48}$$

The z-component of the wavector is given by the usual form $\gamma = [\epsilon_m \omega^2/c^2 - k_{SP}^2]^{1/2}$. With these notations, the field can be cast in the form:

$$\begin{aligned}\mathbf{E} = \int \frac{\mathrm{d}\omega}{2\pi} \int \frac{\mathrm{d}\beta}{2\pi} \Big[& E_>(\beta, \omega, x) \left(\hat{\mathbf{K}}^+ - \frac{K_{SP}}{\gamma_m}\mathbf{n}_m \right) e^{i(K_{x,SP}x + \beta y + \gamma_m |z| - \omega t)} \\ & + E_<(\beta, \omega, x) \left(\hat{\mathbf{K}}^- - \frac{K_{SP}}{\gamma_m}\mathbf{n}_m \right) e^{i(-K_{x,SP}x + \beta y + \gamma_m |z| - \omega t)} \Big]\end{aligned} \tag{4.49}$$

where $\hat{\mathbf{K}}^+ = (K_{x,SP}\hat{\mathbf{x}} + \beta\hat{\mathbf{y}})/K_{SP}$ and $\hat{\mathbf{K}}^- = (-K_{x,SP}\hat{\mathbf{x}} + \beta\hat{\mathbf{y}})/K_{SP}$. Note that the *modes amplitudes depend on* x. A proper mode representation should use only fixed amplitudes. This is possible if all the sources lie in the $x < 0$ region and the region of interest is the $x > 0$ region. It can be shown in that case that the surface plasmon field can be cast in the form:

$$\mathbf{E} = \int \frac{\mathrm{d}\omega}{2\pi} \int \frac{\mathrm{d}\beta}{2\pi} \left(\hat{\mathbf{K}} - \frac{K_{SP}}{\gamma_m}\mathbf{n}_m \right) E_>(\beta, \omega) e^{i(\mathbf{K}\cdot\mathbf{r} + \gamma_m |z| - \omega t)}. \tag{4.50}$$

where $\mathbf{K} = K_{x,SP}\hat{\mathbf{x}} + \beta\hat{\mathbf{y}}$ is complex and $\hat{\mathbf{K}} = \mathbf{K}/K_{SP}$. We conclude that *stationary monochromatic fields excited by sources confined in a bounded domain are well described out of this domain by a representation that uses complex wavevectors and real frequencies*.

Complex ω or Complex K? A Simple Prescription

To summarize, we have shown that the surface plasmon field can be represented using modes that have either a complex frequency or a complex wavevector. However, these modes amplitudes may still depend on either time or space in the more general case. However, there are two cases where these modes with a complex wavevector or complex frequency can be used with amplitudes which are constant. The first case is the representation of a field excited by a pulse for times after the end of the excitation. Then a representation with modes having a complex frequency is possible. The second case is a field excited by a stationary but localized source. Then a representation using complex wavevectors is possible. To each situation corresponds a specific dispersion relation. This simple analysis yields a simple prescription to choose the proper dispersion relation. Note that in the case of pulses limited in space, both representations can be used.

4.9.3 Implications for LDOS

Let us now discuss the Local Density of States (LDOS). We have already pointed out the connection between the dispersion relation and the LDOS in Sect. 4.8.2. In particular, we have seen that the density of states diverges when the group velocity goes to zero. A quick look at Fig. 4.5 shows that different dispersion relations seem to predict different LDOS. While Fig. 4.5b predicts a very large peak at $\omega_{sp}/\sqrt{2}$ due to the asymptote (zero group velocity) and no states above this frequency, Fig. 4.5a predicts a smaller peak and a non-zero LDOS between $\omega_{SP}/\sqrt{2}$ and ω_{SP}. There must be a unique answer as the LDOS determines the energy density at equilibrium and the lifetime of emitters which are well-defined physical quantities. Again, we see that a prescription is needed to choose the right dispersion relation.

A standard procedure to derive the DOS in the reciprocal space is based on the periodic boundary conditions. Assuming a surface of side L, the wavevector takes the form $\mathbf{K} = n_x \frac{2\pi}{L}\hat{\mathbf{x}} + n_y \frac{2\pi}{L}\hat{\mathbf{y}}$. When performing this analysis, both K_x and K_y are real. Thus *the relevant representation uses real wavevectors and complex frequencies*. The corresponding *dispersion relation has no backbending* and therefore presents a singularity. This is in agreement with another approach of the LDOS based on the use of the Green's tensor that predicts an asymptotic behaviour proportional to $1/(z^3|\epsilon + 1|^2)$ [32, 33]. Of course, this divergence is nonphysical. It is related to the modelling of the medium using a continuous description of the metal without accounting for the non-locality.

4.9.4 Implications for Superresolution and Strong Confinment

Let us first discuss the issue of resolution when imaging with a surface plasmon driven at frequency ω by an external source. If the dispersion curve with the asymptotic behaviour is chosen, there seems to be no diffraction limit (if we neglect the

cut-off due to Landau damping) and only the amplitude decay of surface plasmon due to Ohmic losses in the metal limits the resolution. The effect of the backbending of surface plasmon dispersion discussed in Ref. [46] limits the surface plasmon wavelength $2\pi/\Re(k_{SP})$ and therefore, the resolution. Clearly, both dispersion relations do not lead to the same conclusion and a prescription to choose one or the other is needed. Let us consider a situation where a surface plasmon is excited locally by a stationary monochromatic field. From Sect. 4.9.2, we know that it is valid to use a representation with fixed amplitudes using modes with complex wavevectors and real frequencies. This implies that the dispersion relation with real frequency (with backbending) is relevant. Hence, there is a cut-off spatial frequency. Indeed, as K_x may be complex, the propagation term $\exp(i K_x x)$ introduces damping. In the case of a lossy medium, damping may be due to losses. However, even for a non-lossy medium (k_{SP} is real), $K_x = (k_{SP}^2 - \beta^2)^{1/2}$ can be imaginary. This occurs when β exceeds the value K_{SP}. This situation is the 2D analogue of the evanescent waves with wavevector K larger than ω/c that cannot propagate in a vacuum. Clearly, k_{SP} is a cut-off frequency and the propagation term $\exp(i K_x x)$ works as a low-pass filter that prevents the propagation of fields associated with spatial frequencies larger than k_{SP}. When dealing with lossy media, it is the real part of k_{SP} that specifies the cut-off spatial frequency. It is seen in Fig. 4.5 that this real part is limited by the backbending of the dispersion relation.

In summary, when discussing *imaging with stationary monochromatic surface plasmons, the relevant representation is based on modes with a complex wavector and a real frequency* given by Eq. (4.50). This corresponds to a *dispersion relation with a backbending*. It follows that *the resolution is limited* by the cut-off spatial frequency given by the maximum value of $\Re(k_{SP})$.

4.10 Fourier Optics for SPP

In this section, we study the propagation of surface plasmon polaritons along a flat interface. Several experiments demonstrating propagation, interferences and diffraction by surface plasmons have been reported in the literature [93–97]. In usual optics, these phenomena are well described in the framework of optical physics, which is based on the Huygens–Fresnel principle. In this section, we derive an analogue of this principle for surface plasmons following Ref. [98]. We consider the propagation of a monochromatic surface plasmon field along a planar surface $z = 0$ in the direction of positive x. We assume that the field is known at $x = 0$ and we seek an expression of the field for $x > 0$. If a Huygens–Fresnel-type approach can be used, we expect to be able to assume that each point along the line $x = 0$ acts as a secondary source that radiates a cylindrical wave.

4.10.1 General Representation

The general representations of the field given in Sect. 4.9.2 provide the adequate formalism to deal with these phenomena. In particular, Eq. (4.50) is a rigorous form of the surface plasmon field valid in a region with no sources. Let us stress that this representation is valid for a complex wavevector $\mathbf{K}$ and a real frequency ω so that this representation is necessarily associated with a dispersion relation with backbending. We emphasize that this representation is well suited to discuss propagation for $x > x_0$ of a surface plasmon field known along a line $x = x_0$. It is seen in Eq. (4.50) that propagation over a distance d amounts to multiply the amplitude of each mode by a factor $\exp(ik_{x,SP}d)$. In general, this involves modifying both the phase and the amplitude of the mode. Thus, it allows us to discuss any surface wave diffraction problem. Hereafter, the time dependence $\exp(-i\omega t)$ will be omitted for brevity. From Eq. (4.50), we have:

$$\mathbf{E}^{SP}(x,y) = \int \frac{d\beta}{2\pi}\, \mathbf{E}^{SP}(\beta) e^{i\sqrt{k_{SP}^2-\beta^2}x+i\beta y}. \tag{4.51}$$

This expansion is analogous to the angular plane wave representation of fields in a vacuum. It is valid for $x > 0$ in a source free region. Note that we have omitted the z-dependence of the field given by $\exp(i\sqrt{\epsilon_1\omega^2/c^2 - k_{SP}^2}\, z)$ in the upper medium and by $\exp(-i\sqrt{\epsilon_2\omega^2/c^2 - k_{SP}^2}\, z)$ in the metal. Indeed, the decay along the z-axis depends on the frequency but not on β.

A first simplification arises when reducing the problem to a scalar problem. Indeed, it turns out that the x- and y-components of the electric field can be derived from the form of the z-component of the electric field. This is a straightforward consequence of $\operatorname{div}\mathbf{E} = 0$ so that $\mathbf{K}\cdot\mathbf{E} + k_z E_z = 0$. The electric field components are thus given by:

$$\begin{aligned} E_x(\beta) &= \sqrt{k_{SP}^2-\beta^2}\,\frac{k_z}{k_{SP}^2} E_z^{SP}(\beta) \\ E_y(\beta) &= k_y \frac{k_z}{k_{SP}^2} E_z^{SP}(\beta) \\ E_z^{SP}(\beta), & \end{aligned} \tag{4.52}$$

where $k_z = \sqrt{\epsilon_1\omega^2/c^2 - k_{SP}^2}$ is the z-component of the wavevector in dielectric environment.

4.10.2 Huygens–Fresnel Principle

We now proceed to derive a vectorial form of the Huygens principle with no approximation. Note in particular that the result will account for polarization and near-field effects. We observe that the integral in Eq. (4.51) is the Fourier transform of the product of two functions of β. For example, for the z-component, we have:

$$E_z^{SP}(x, y) = \int \frac{\mathrm{d}\beta}{2\pi} \left[E_z^{SP}(\beta)\right] \left[e^{i\sqrt{k_{SP}^2 - \beta^2}x}\right] e^{i\beta y}. \tag{4.53}$$

The integral can thus be written as a convolution product of the Fourier transforms of $E_z^{SP}(\beta)$ and $\exp(i\sqrt{k_{SP}^2 - \beta^2}x)$. Making use of the integral representation of the Hankel function, we obtain:

$$\int \mathrm{d}\beta \left[e^{i\sqrt{k_{SP}^2 - \beta^2}x}\right] e^{i\beta y} = -i\pi \frac{\partial}{\partial x} H_0^{(1)}(k_{SP}\rho)$$

where $\rho = \sqrt{x^2 + y^2}$. Equation (4.53) can thus be cast in the form:

$$E_z^{SP}(x, y) = \frac{-i}{2} \int \mathrm{d}y' \; E_z^{SP}(x = 0, y') i \frac{\partial}{\partial x} H_0^{(1)}(k_{SP}\rho). \tag{4.54}$$

Similarly, we find:

$$E_x^{SP}(x, y) = \frac{-1}{2} \int \mathrm{d}y' \; E_z^{SP}(x = 0, y') \frac{k_z}{k_{SP}^2} \frac{\partial^2}{\partial x^2} H_0^{(1)}(k_{SP}\rho), \tag{4.55}$$

and:

$$E_y^{SP}(x, y) = \frac{-1}{2} \int \mathrm{d}y' \; E_z^{SP}(x = 0, y') \frac{k_z}{k_{SP}^2} \frac{\partial^2}{\partial x \partial y} H_0^{(1)}(k_{SP}\rho). \tag{4.56}$$

Equation (4.54) can be viewed as a vectorial Huygens–Fresnel principle for surface plasmons. Indeed, the surface plasmon field at (x, y) appears to result from the interferences of surface plasmons emitted by secondary sources located at $(x = 0, y')$ with an amplitude $E_z^{SP}(x = 0, y')$. In order to see more clearly the link with Huygens–Fresnel principle, we use the asymptotic form of the Hankel function, valid for distances larger than the wavelength. We obtain:

$$E_z^{SP}(x, y) = -\frac{i}{\sqrt{\lambda_{SP}}} \int \mathrm{d}y' \; \cos\theta \; E_z^{SP}(x = 0, y') \frac{e^{ik_{SP}\rho}}{\sqrt{\rho}} e^{i\pi/4}, \tag{4.57}$$

where $\lambda_{SP} = 2\pi/k_{SP}$ is the surface plasmon wavelength and $\theta = \arccos(x/\rho)$. Here, the propagator is a damped cylindrical wave $e^{ik_{SP}\rho}/\sqrt{\rho}$ instead of the

spherical wave e^{ikr}/r in the case of light propagation in a 3D vacuum. We recover in this asymptotic regime a surface plasmon form that has been conjectured previously [99, 96]. However, let us emphasize two differences between the scalar approximation and the propagator given by Eq. (4.54). Firstly, Eq. (4.54) is valid for any distance and includes near-field terms. Secondly, Eqs. (4.55) and (4.56) show that the x- and y-components of the electric field can be derived from the z-component. More specifically, the parallel components of the field are given by $E_x = \frac{k_z}{k_{SP}^2}\frac{\partial E_z}{\partial x}$, $E_y = \frac{k_z}{k_{SP}^2}\frac{\partial E_z}{\partial y}$.

4.11 Conclusion

After more than 50 years, surface plasmons are still a very active research area. There has been a remarkable increase of novel results in the last ten years, mostly due to the simultaneous progress in observation and fabrication techniques. Observation techniques are reviewed in a separate chapter. They have made tremendous progress since the first near-field microscopy image [100] of a surface plasmon. The progress of nanofabrication makes possible the control of nanostructures that can take full advantage of the potential of surface plasmons. It is the purpose of this introductory chapter to highlight the polaritonic aspect of surface plasmons, or in other words, its dual electronic and electromagnetic nature. Surface plasmons are becoming a very important tool for the control of optical fields at the nanoscale. I believe that it is important to be aware of the underlying microscopic nature of surface plasmons in order to fully appreciate their potential and limitations.

References

1. L.M. Brekhovskikh, Waves in layered media (Academic Press, New York, 1960)
2. A. Banos, *Dipole radiation in the presence of a conducting half-space* (IEEE Press, Piscataway, 1994)
3. L. Felsen, N. Marcuvitz, *Radiation and scattering of waves* (Oxford University Press, NY, 1996)
4. R.W.P. King, M. Owens, T.T. Wu, *Lateral electromagnetic waves* (Springer Verlag, NY, 1992)
5. A.D. Boardman(ed.), Electromagnetic surface modes (Wiley, New York, 1982)
6. V.M. Agranovich, D.L. Mills (eds.), *Surface Polaritons* (North-Holland, Amsterdam, 1982)
7. H. Raether, *Surface Plasmons* (Springer-Verlag, Berlin, 1988)
8. A.V. Zayats, I.I. Smolyaninov, A.A. Maradudin, Phys. Rep. **408**, 131 (2005)
9. W.L. Barnes, A. Dereux, T.W. Ebbesen, Nature **424**, 824 (2003)
10. J.A. Schuller, E.S. Barnard, W. Cai, Y.C. Jun, J.S. White, M.L. Brongersma, Nat. Mater. **9**, 193 (2010)
11. C. Kittel, *Solid State Physics* (John Wiley, New York, 1987)
12. N.W. Ashcroft, N.D. Mermin, *Solid State Physics* (Holt-Saunders, New York, 1976)
13. J.M. Ziman, *Principles of the theory of solids* (Cambridge University Press, London, 1964)

14. D. Pines, *Elementary excitations in solids: lectures on phonons, electrons and plasmons* (W.A. Benjamin, London, 1964)
15. C. Kittel, *Quantum Theory of Solids* (Wiley, New York, 1987)
16. J.D. Jackson, *Classical Electrodynamics*, 3rd edn. (Wiley, New York, 1999)
17. G.W. Ford, W.H. Weber, Phys. Rep. **113**, 195 (1984)
18. L.D. Landau, L.P. Pitaevskii, E.M. Lifshitz, *Electrodynamics of continuous media* (Elsevier, Amsterdam, 2004)
19. P.G. Etchegoin, E.C. Le Ru, M. Meyer, J. Chem. Phys. **125**, 164705 (2006)
20. M. Ordal et al., Appl. Opt. **24**, 4493 (1985)
21. N. Del Fatti, Ph.D Dissertation, Ecole Polytechnique, 1999
22. M. Kaveh, N. Wiser, Adv.in Phys. **33**, 257 (1984)
23. C. Yi Tsai, C. Yao Tsai, C.H. Chen, T.L. Sung, T.Y. Wu, F.P. Shih, IEEE J. Quantum. Electron. **34**, 552 (1998)
24. P.B. Allen, Phys. Rev. B **3**, 305 (1971)
25. J.B. Smith, H. Ehrenreich, Phys. Rev. B **25**, 923 (1982)
26. R.N. Gurzhi, M. Ya Azbel', H.P. Lin, Sov. Phys. Solid State **5**, 554 (1963)
27. A. Vial, A.S. Grimault, D. Macias, D. Barchiesi, M. Lamy de la Chapelle, Phys. Rev. B **71**, 085416 (2005)
28. T. Laroche, C. Girard, Appl. Phys. Lett. **89**, 233119 (2006)
29. F. Hao, P. Nordlander, Chem. Phys. Lett. **446**, 115 (2007)
30. P.B.Johnson, R.W.Christy, Phys. Rev. B **6**, 4370 (1972)
31. A.V. Shchegrov, K. Joulain, R. Carminati, J.J. Greffet, Phys. Rev. Lett. **85**, 1548 (2000)
32. K. Joulain, R. Carminati, J.P. Mulet, J.J. Greffet, Phys. Rev. B **68**, 245405 (2003)
33. K. Joulain, J.P. Mulet, F. Marquier, R. Carminati, JJ Greffet. Surf. Sci. Rep. **57**, 59 (2005)
34. R.E. Collin, IEEE Trans. Antennas Propag. Mag. **46**, 64 (2004)
35. P. Lalanne, J.P. Hugonin, Nat. Phys. **2**, 551 (2006)
36. P. Lalanne, J.P. Hugonin, H.T. Liu, B. Wang, Sur. Sci. Rep. **64**, 453 (2009)
37. H. Liu, P. Lalanne, Nature **452**, 728 (2008)
38. W. Dai, C.M. Soukoulis, Phys. Rev. B **80**, 155407 (2009)
39. A. Yu Nikitin, S.G. Rodrigo, F.J. Garcia-Vidal, L. Martin-Moreno, New J. Phys. **11**, 123020 (2009)
40. K. Aki, P.G. Richards, *Quantitative Seismology* (University Science Books, Sausalito, 2002)
41. J.B. Pendry, Phys. Rev. Lett. **85**, 3966 (2000)
42. N. Fang, H. Lee, C. Sun and X. Zhang. Science **308**, 534 (2005)
43. T. Taubner, D. Korobkin, Y. Urzhumov, G. Shvets, R. Hillenbrand, Science **313**, 1595 (2006)
44. I.I. Smolyaninov, C.C. Davis, A.V. Zayats, New J. Phys. **7**, 175(1)–175(7) (2005)
45. I.I. Smolyaninov, C.C. Davis, J. Elliot, A.V. Zayats, Phys. Rev. Lett. **98**, 209704 (2007)
46. A. Drezet, A. Hohenau, J.R. Krenn, Phys. Rev. Lett. **98**, 209703 (2007)
47. D.W. Pohl, W. Denk, M. Lanz, Appl. Phys. Lett. **44**, 651 (1984)
48. A. Lewis, M. Isaacson, A. Harootunian, A. Murray, Ultramicroscopy **13**, 227 (1984)
49. H.J. Lezec, A. Degiron, E. Devaux, R.A. Linke, L. MArtin-Poreno, F.J. Garcia-Vidal, T.W. Ebbesen, Science **297**, 820 (2002)
50. J. Wessel, J. Opt. Soc. Am. B **2**, 1538 (1985)
51. A. Madrazo, R. Carminati, M. Nieto-Vesperinas, J.J. Greffet, J. Opt. Soc. Am. A **15**, 109 (1998)
52. K. Li, M.I. Stockman, D.J. Bergman, Phys. Rev. Lett. **91**, 227402 (2003)
53. Y.C. Jun, R.D. Kekatpure, J.S. White, M.L. Brongersma, Phys. Rev. B **78**, 153 111 (2008)
54. S.I. Bozhevolnyi, V.S. Vokov, E. Devaux, JY Laluet and T. Ebbesen, Nature **440**, 508 (2006)
55. R. Esteban, T. Teperik, JJ Greffet. Phys. Rev. Lett. **104**, 026802 (2010)
56. Y. Todorov, A.M. Andrews, R. Colombelli, S. de Liberato, C. Ciuti, P. Klang, G. Strasser, C. Sirtori, Phys. Rev. Lett. **105**, 196402 (2010)
57. K.H. Drexhage, *in Progress in Optics* (Ed. E. Wolf, North Holland, Amsterdam, 1974)
58. R.R. Chance, A. Prock, R. Silbey, Adv. Chem. Phys. **37**, 1 (1978)
59. W.L. Barnes, J. Mod. Opt. **45**, 661 (1998)

60. E. Rousseau, A. Siria, G. Jourdan, S. Volz, F. Comin, J. Chevrier, JJ Greffet. Nat. Photonics **3**, 514 (2006)
61. Y. de Wilde, F. Formanek, R. Carminati, B. Gralak, PA Lemoine, K. Joulain, JP Mulet, Y. Chen, JJ Greffet. Nature **444**, 740 (2006)
62. J.P. Mulet, K. Joulain, R. Carminati, J.J. Greffet, Nanoscale Microscale Thermophys. Eng. **6**, 209 (2002)
63. J.P. Mulet, K. Joulain, R. Carminati, J.J. Greffet, Appl. Phys. Lett. **78**, 2931 (2001)
64. S. Shen, A. Narayanaswamy, G. Chen, Nano Lett. **9**, 2909 (2009)
65. S.A. Biehs, E. Rousseau, JJ Greffet. Phys. Rev. Lett. **105**, 234301 (2010)
66. J.M. Gérard, B. Gayral, J. Lightwave Technol. **17**, 2089 (1999)
67. J.J. Greffet, M. Laroche, F. Marquier. Phys. Rev. Lett. **105**, 117701 (2010)
68. S. Haroche, in Proceedings of the Les Houches Summer School Fundamentals Systems in Quantum Optics, Elsevier Science Publishers, Amsterdam, 1992, ed. by J. Dalibard
69. A. Kock, E. Gornik, M. Hauser, W. Beistingl, Appl. Phys. Lett. **57**, 2327 (1990)
70. D.K. Gifford, D.G. Hall, Appl. Phys. Lett. **81**, 4315 (2002)
71. J. Azoulay, A. Débarre, A. Richard, P. Tchénio, Europhys. Lett. **51**, 374 (2000)
72. M. Thomas, JJ Greffet, R. Carminati, JR Arias-Gonzalez. Appl. Phys. Lett. **85**, 3863 (2004)
73. K. Okamoto, I. Niki, A. Shvartser, Y Narukawa, T. Mukai, A. Scherer. Nat. Mater. **3**, 601 (2004)
74. S. Kuhn, Ulf Hakanson, L. Rogobete, V. Sandoghdar. Phys. Rev. Lett. **97**, 017402 (2006)
75. P. Anger, P. Bharadwaj, L. Novotny, Phys. Rev. Lett. **96**, 113002 (2006)
76. A. Curto, G. Volpe, T.H. Taminiau, M.P. Freuzer, R. Quidant, N.F. van Hulst, Science **329**, 930 (2010)
77. T.H. Taminiau, F.D. Stefani, F.B. Segerink, N.F. van Hulst, Nat. Photonics **2**, 234 (2008)
78. H.B.G. Casimir, Proc. Koninkl. Ned. Akad. Wetenschap. **51**, 793 (1948)
79. S.K. Lamoreaux, Phys.rev.Lett. **78**, 5 (1997)
80. R.S. Decca, D. Lopez, E Fishbach, DE Krause. Phys. Rev. Lett. **91**, 050402 (2003)
81. G. Jourdan, A. Lambrecht, F. Comin, J. Chevrier, Europhys. Lett. **85**, 31001 (2009)
82. C. Genet, A. Lambrecht, S. Reynaud, Phys. Rev.A **62**, 012110 (2000)
83. C. Henkel, K. Joulain, J.P Mulet, J.J Greffet, Phys. Rev.A **69**, 023808 (2004)
84. F. Intravaia, A. Lambrecht, Phys. Rev. Lett. **94**, 110404 (2005)
85. F. Intravaia, C. Henkel, A. Lambrecht, Phys. Rev.A **76**, 033820 (2007)
86. M.I. Stockman, S.V. Faleev, D.J. Bergman, Phys. Rev. Lett. **88**, 067402 (2002)
87. M. Aeschlimann et al., Nature **446**, 301 (2007)
88. D. Sarid, Phys. Rev. Lett. **47**, 1927 (1981)
89. E. Prodan, C. Radloff, N.J. Halas, P. Nordlander, Science **302**, 419 (2003)
90. A. Archambault, T. Teperik, F. Marquier, J.J. Greffet, Phys. Rev. B **79**, 195414 (2009)
91. R.W. Alexander, G.S. Kovener, R.J. Bell, Phys. Rev. Lett. **32**, 154 (1974)
92. E.T. Arakawa, M.W. Williams, R.N. Hamm, R.H. Ritchie, Phys. Rev. Lett. **31**, 1127 (1973)
93. L. Feng, K.A. Tetz, B. Slutsky, V. Lomakin, Y. Fainman Appl, Phys. Lett. **91**, 081101 (2007)
94. Z. Liu, J.M. Steele, W. Srituravanich, Y. Pikus, C. Sun, X. Zhang, Nano Lett. **5**, 1726–1729 (2005)
95. L. Yin, V.K. Vlasko-Vlasov, J. Pearson, J.M. Hiller, J. Hua, U. Welp, D.E. Brown, C.W. Kimball, Nano Lett. **5**, 1399–1402 (2005)
96. A.J. Huber, B. Deutsch, L. Novotny, R. Hillenbrand, Appl. Phys. Lett. **92**, 203104 (2008)
97. R. Zia, M.L. Brongersma, Nat. Nanotechnol. **2**, 426–429 (2007)
98. T.V. Teperik, A. Archambault, F. Marquier, J.J. Greffet, Opt. Express **17**, 17483 (2009)
99. I.I. Smolyaninov, D.L. Mazzoni, J. Mait, C.C. Davis, Phys. Rev. B **56**, 1601 (1997)
100. P. Dawson, F. de Fornel, J.P. Goudonnet, Phys. Rev. Lett. **72**, 2927 (1994)